

UC Davis

UC Davis Previously Published Works

Title

Selectin-targeting glycosaminoglycan-peptide conjugate limits neutrophil-mediated cardiac reperfusion injury

Permalink

<https://escholarship.org/uc/item/4x10q4hr>

Journal

Cardiovascular Research, 118(1)

ISSN

0008-6363

Authors

Dehghani, Tima

Thai, Phung N

Sodhi, Harkanwalpreet

et al.

Publication Date

2022-01-07

DOI

10.1093/cvr/cvaa312

Peer reviewed

Cardiovascular Research

Selectin-Targeting Glycosaminoglycan-Peptide Conjugate Limits Neutrophil Mediated Cardiac Reperfusion Injury --Manuscript Draft--

Manuscript Number:	CVR-2020-0408R2
Full Title:	Selectin-Targeting Glycosaminoglycan-Peptide Conjugate Limits Neutrophil Mediated Cardiac Reperfusion Injury
Short Title:	Glycocalyx mimic limits cardiac reperfusion injury
Article Type:	Original Article
Keywords:	inflammation; myocardial infarction; endothelial cell dysfunction; Fibrosis; glycocalyx
Corresponding Author:	Alyssa Panitch University of California Davis Davis, CA UNITED STATES
Corresponding Author Secondary Information:	
Corresponding Author's Institution:	University of California Davis
Corresponding Author's Secondary Institution:	
First Author:	Alyssa Panitch
First Author Secondary Information:	
Order of Authors:	Alyssa Panitch Tima Dehghani Phung N. Thai Harkanwalpreet Sodhi Lu Ren Padmini Sirish Carol E. Nader Valeriy Timofeyev James L Overton Xiaocen Li Kit S. Lam Nipavan Chiamvimonvat
Order of Authors Secondary Information:	
Abstract:	<p>Aims: One of the hallmarks of myocardial infarction (MI) is excessive inflammation. During an inflammatory insult, damaged endothelial cells shed their glycocalyx, a carbohydrate-rich layer on the cell surface which provides a regulatory interface to immune cell adhesion. Selectin-mediated neutrophilia occurs as a result of endothelial injury and inflammation. We recently designed a novel selectin-targeting glycocalyx mimetic (termed DS-IkL) capable of binding inflamed endothelial cells. This study examines the capacity of DS-IkL to limit neutrophil binding and platelet activation on inflamed endothelial cells, as well as the cardio-protective effects of DS-IkL after acute myocardial infarction.</p> <p>Methods and Results : In vitro , DS-IkL diminished neutrophil interactions with both recombinant selectin and inflamed endothelial cells , and limited platelet activation on inflamed endothelial cells. Our data demonstrated that DS-IkL localized to regions of vascular inflammation in vivo after 45 minutes of left anterior descending coronary</p>

artery ligation induced MI. Further, findings from this study show DS-IkL treatment was cardioprotective by diminishing neutrophil and platelet-mediated injury. Mice treated with DS-IkL immediately after ischemia/reperfusion and 24 hours later exhibited reduced neutrophil extravasation, macrophage accumulation, fibroblast and endothelial cell proliferation, and fibrosis compared to saline controls.

Conclusions: Our findings suggest that DS-IkL has great therapeutic potential after MI by limiting reperfusion injury induced by the immune response.

Translational Perspective: Cardiovascular disease remains the leading cause of mortality worldwide. Acute inflammation from myocardial infarction (MI) results in damaged endothelial cells, leading to the loss of glycocalyx. Here, we designed a novel selectin-targeting glycocalyx mimetic (termed DS-IkL) capable of binding inflamed endothelial cells. DS-IkL limits neutrophil binding and platelet activation on inflamed endothelial cells. Treatment with DS-IkL in a preclinical model of MI reduces infarct size by preventing neutrophil extravasation, macrophage accumulation, fibroblast and endothelial cell proliferation, and fibrosis. Our findings suggest that DS-IkL has great therapeutic potential after MI by limiting reperfusion injury induced by the immune response.

ABSTRACT

Aims: One of the hallmarks of myocardial infarction (MI) is excessive inflammation. During an inflammatory insult, damaged endothelial cells shed their glycocalyx, a carbohydrate-rich layer on the cell surface which provides a regulatory interface to immune cell adhesion. Selectin-mediated neutrophilia occurs as a result of endothelial injury and inflammation. We recently designed a novel selectin-targeting glycocalyx mimetic (termed DS-IkL) capable of binding inflamed endothelial cells. This study examines the capacity of DS-IkL to limit neutrophil binding and platelet activation on inflamed endothelial cells, as well as the cardio-protective effects of DS-IkL after acute myocardial infarction.

Methods and Results: *In vitro*, DS-IkL diminished neutrophil interactions with both recombinant selectin and inflamed endothelial cells, and limited platelet activation on inflamed endothelial cells. Our data demonstrated that DS-IkL localized to regions of vascular inflammation *in vivo* after 45 minutes of left anterior descending coronary artery ligation induced MI. Further, findings from this study show DS-IkL treatment had short- and long-term cardioprotective effects after ischemia/reperfusion at the left anterior descending coronary artery. Mice treated with DS-IkL immediately after ischemia/reperfusion and 24 hours later exhibited reduced neutrophil extravasation, macrophage accumulation, fibroblast and endothelial cell proliferation, and fibrosis compared to saline controls.

Conclusions: Our findings suggest that DS-IkL has great therapeutic potential after MI by limiting reperfusion injury induced by the immune response.

Keywords: inflammation, myocardial infarction, endothelial cell dysfunction, fibrosis, glycocalyx

Translational Perspective

Cardiovascular disease remains the leading cause of mortality worldwide. Acute inflammation from myocardial infarction (MI) results in damaged endothelial cells, leading to the loss of glycocalyx. Here, we designed a novel selectin-targeting glycocalyx mimetic (termed DS-IkL) capable of binding inflamed endothelial cells. DS-IkL limits neutrophil binding and platelet activation on inflamed endothelial cells. Treatment with DS-IkL in a preclinical model of MI reduces infarct size by preventing neutrophil extravasation, macrophage accumulation, fibroblast and endothelial cell proliferation, and fibrosis. Our findings suggest that DS-IkL has great therapeutic potential after MI by limiting reperfusion injury induced by the immune response.

UNIVERSITY OF CALIFORNIA, DAVIS

BERKELEY • DAVIS • IRVINE • LOS ANGELES • MERCED • RIVERSIDE • SAN DIEGO • SAN FRANCISCO



SANTA BARBARA • SANTA CRUZ

DEPARTMENT OF BIOMEDICAL ENGINEERING
UNIVERSITY OF CALIFORNIA, DAVIS
ONE SHIELDS AVENUE
DAVIS, CA 95616

TELEPHONE: (530) 754-6645

FAX: (530) 754-5739

EMAIL: apanitch@ucdavis.edu

October 1, 2020

Professor Tomasz J. Guzik, MD, PhD, FRCP, FACP
Editor-in-Chief, *Cardiovascular Research*
Institute of Cardiovascular and Medical Sciences
University of Glaskow, UK

Dear Editor Guzik:

Thank you for the opportunity to provide a revised manuscript entitled “Selectin-Targeting Glycosaminoglycan-Peptide Conjugate Limits Cardiac Injury After Myocardial Infarction by Abating Neutrophil Recruitment” for consideration for publication *Cardiovascular Research*. We have carefully considered the reviewer’s concerns and modified the manuscript accordingly. The change to the manuscript is done in blue font for ease of identification within the manuscript. It is also described in our response to reviewers.

On behalf of all authors, I attest that this work has not been previously published or submitted elsewhere for publication, nor have any discussions with journal editors occurred regarding the work.

Sincerely,

A handwritten signature in blue ink, appearing to read 'Alyssa Panitch'.

Alyssa Panitch
Edward Teller Professor
Department of Biomedical Engineering
University of California, Davis

We would like to again thank the editors and reviewers for the time they have taken to review our manuscript and to provide critical feedback that has helped improve to manuscript. We have fully addressed each concern below and within the manscript.

Reviewers' comments:

Reviewer #1: The manuscript was well revised.

Thank you

Reviewer #3: No further comments.

Thank you

Reviewer #4: The authors have not adjusted their facs experiments. immunofluorescence images quantifying Ly6G+ cells and F4/80+ cells separately does reinforce the facs data that hinted that some combination of CD11b+, LyC/Ly6G+ (ie mix of myeloid cells) cell numbers are changing. The endothelial and fibroblast facs is very difficult to interpret without CD45 to gate out the hematopoietic cells that CD31 (monocytes, macrophages, T cells) and Thy1+ (all the T cells and some myeloid cells)---this is not a major point in the papers, so if the authors can not do further experiments, they need to acknowledge the caveats of this interpretation in the text.

We understand and agree with your concern. We have acknowledged the limitations of the study in the discussion be adding the following statement (lines 441-444).

It must be noted that CD45 was not used to gate out hematopoietic cells that may also be positive for CD31 or Thy1.2+. Thus, while the changes in endothelial and fibroblast cell numbers are suggestive, future work is needed to definitively show these changes.

Selectin-Targeting Glycosaminoglycan-Peptide Conjugate Limits Neutrophil Mediated Cardiac Reperfusion Injury

Tima Dehghani^{1*}, Phung N. Thai^{2*}, Harkanwalpreet Sodhi¹, Lu Ren², Padmini Sirish², Carol E. Nader², Valeriy Timofeyev², James L. Overton², Xiaocen Li³, Kit S. Lam³, Nipavan Chiamvimonvat^{2,4,5}, Alyssa Panitch¹

¹Department of Biomedical Engineering, University of California, Davis

²Department of Internal Medicine, Division of Cardiovascular Medicine, University of California, Davis

³Department of Biochemistry and Molecular Medicine, University of California, Davis

⁴Department of Veterans Affairs, Northern California Health Care System, Mather, CA

⁵Department of Pharmacology, University of California, Davis

*Authors contributed equally to this project

Short Title: Glycocalyx mimic limits cardiac reperfusion injury

To whom correspondence should be addressed:

Alyssa Panitch
Department of Biomedical Engineering
University of California, Davis
451 Health Sciences Drive, GBSF 2303
Davis, CA 95616
Email: apanitch@ucdavis.edu

Manuscript Category: Original article

Total Words: 9207

ABSTRACT

1 **Aims:** One of the hallmarks of myocardial infarction (MI) is excessive inflammation. During an
2 inflammatory insult, damaged endothelial cells shed their glycocalyx, a carbohydrate-rich layer on
3 the cell surface which provides a regulatory interface to immune cell adhesion. Selectin-mediated
4 neutrophilia occurs as a result of endothelial injury and inflammation. We recently designed a
5 novel selectin-targeting glycocalyx mimetic (termed DS-IkL) capable of binding inflamed
6 endothelial cells. This study examines the capacity of DS-IkL to limit neutrophil binding and
7 platelet activation on inflamed endothelial cells, as well as the cardio-protective effects of DS-IkL
8 after acute myocardial infarction.

9 **Methods and Results:** *In vitro*, DS-IkL diminished neutrophil interactions with both recombinant
10 selectin and inflamed endothelial cells, and limited platelet activation on inflamed endothelial
11 cells. Our data demonstrated that DS-IkL localized to regions of vascular inflammation *in vivo*
12 after 45 minutes of left anterior descending coronary artery ligation induced MI. Further, findings
13 from this study show DS-IkL treatment had short- and long-term cardioprotective effects after
14 ischemia/reperfusion at the left anterior descending coronary artery. Mice treated with DS-IkL
15 immediately after ischemia/reperfusion and 24 hours later exhibited reduced neutrophil
16 extravasation, macrophage accumulation, fibroblast and endothelial cell proliferation, and fibrosis
17 compared to saline controls.

18 **Conclusions:** Our findings suggest that DS-IkL has great therapeutic potential after MI by limiting
19 reperfusion injury induced by the immune response.

Keywords: inflammation, myocardial infarction, endothelial cell dysfunction, fibrosis, glycocalyx

Translational Perspective

20 Cardiovascular disease remains the leading cause of mortality worldwide. Acute
21 inflammation from myocardial infarction (MI) results in damaged endothelial cells, leading to the
22 loss of glycocalyx. Here, we designed a novel selectin-targeting glycocalyx mimetic (termed DS-
23 IkL) capable of binding inflamed endothelial cells. DS-IkL limits neutrophil binding and platelet
24 activation on inflamed endothelial cells. Treatment with DS-IkL in a preclinical model of MI
25 reduces infarct size by preventing neutrophil extravasation, macrophage accumulation, fibroblast
26 and endothelial cell proliferation, and fibrosis. Our findings suggest that DS-IkL has great
27 therapeutic potential after MI by limiting reperfusion injury induced by the immune response.

28

29

INTRODUCTION

30 Cardiovascular disease remains the leading cause of mortality in the United States.
31 Approximately 805,000 Americans will be diagnosed with coronary artery disease (CAD), the
32 most common heart disease, this year¹. Approximately half of those diagnosed with CAD will be
33 susceptible to acute myocardial infarction (MI), as well as complications that can lead to heart
34 failure and sudden cardiac death². Although initial damage occurs during acute MI due to oxygen
35 deprivation during the ischemic phase, it is well documented that further injury can result from
36 reperfusion³. The effects of reperfusion injury (RI) are complex. In the absence of oxygen,
37 ischemic tissues experience severe disruptions to their homeostasis. A necessary shift from aerobic
38 to anaerobic metabolism results in the accumulation of lactic acid, which contributes to a decline
39 in intracellular pH, an impairment of ion exchange, and an increase in reactive oxygen species
40 (ROS) production^{3, 4}, subsequently damaging cells within the vicinity. Paradoxically, the
41 restoration of blood flow further contributes to cellular damage, partly due to inefficient oxidative

42 phosphorylation that results in further production of ROS, reductions in nitric oxide (NO), and the
43 recruitment of immune cells^{5, 6}.

44 Ischemia/reperfusion induced damage to vascular endothelial cells (EC) initiates an
45 inflammatory cascade that recruits neutrophils and platelets to the sites of damage⁵. Increased
46 permeability of the vasculature potentiates RI by allowing the infiltration of immune cells into the
47 tissue. Reperfused ECs experience disruptions to their Ca²⁺ homeostasis and begin to contract⁷,
48 giving rise to endothelial gaps that facilitate the extravasation of leukocytes being recruited by
49 ROS and cytokines. Though these cells have vital cardioprotective functions, overaccumulation of
50 leukocytes and activated platelets exacerbates myocardial damage, contributing to the overall
51 infarct size.

52 During RI, ECs shed their glycocalyx, a carbohydrate-rich protective layer that resides on
53 the surface of healthy endothelium^{8, 9}. The glycocalyx is known to play a role in many cellular
54 processes, including mechanotransduction¹⁰, microvascular permeability¹¹, and modulation of
55 inflammatory mediators¹². Diminution of the endothelial glycocalyx has been shown to contribute
56 to vascular edema as well as neutrophil and platelet adhesion^{13, 14}. While the endothelial glycocalyx
57 has been shown to recover from enzyme-induced damage, this recovery was inversely proportional
58 to white blood cell count¹⁵. The inflammatory response hence plays a critical role in RI with respect
59 to the glycocalyx, with neutrophil influx^{16, 17} and increased enzyme production^{8, 18} likely delaying
60 glycocalyx regeneration. Therefore, a molecule that provides a stable, stealthy interface with the
61 capacity to down-regulate platelet activation and neutrophil capture could prevent inflammation-
62 mediated RI.

63 To address this critical problem, we have designed a novel multivalent selectin-targeting
64 carbohydrate conjugate (termed DS-IkL) that effectively abates neutrophil interactions within

65 damaged regions of the vasculature. Given the elevated levels of matrix metalloproteinases and
66 other proteolytic enzymes within the inflammatory zone, the glycosaminoglycan-derived
67 backbone is conjugated to several selectin binding peptides consisting of D- or unnatural amino
68 acids in order to increase the enzymatic stability of the molecule in the harsh inflammatory
69 environment. We directly test the hypothesis that DS-IkL will significantly interfere with
70 neutrophil capture and platelet activation on ECs *in vitro*, and provide beneficial effects *in vivo* in
71 a preclinical model of MI by reducing neutrophil extravasation, macrophage accumulation,
72 fibroblast and EC proliferation, and fibrosis.

73 Our study demonstrates that DS-IkL interfered with neutrophil capture and adhesion on E-
74 selectin substrates and cytokine stimulated cardiac-derived ECs. DS-IkL provided a protective
75 effect against platelet activation on ECs *in vitro*, maintaining a similar activation state as on
76 unstimulated ECs. In corroboration with these findings, we observed cardioprotection after a left
77 anterior descending coronary artery (LAD) ligation-induced MI in mice *in vivo*. Treatment with
78 DS-IkL resulted in improved cardiac function, reduced fibrosis, and a significant decrease in
79 neutrophil, macrophage, proliferative fibroblasts, and proliferative ECs in the infarcted region.
80 Taken together, these findings establish a therapeutic role of DS-IkL after MI by reducing
81 reperfusion injury mediated by the immune response.

82

83 MATERIALS AND METHODS

84 For more detailed methods, please see **Supplementary Materials**.

85 **Animal Model / IR Surgery**

86 We used 10-16 week-old male and female C57Bl/6J mice for this study. All animal
87 handling and laboratory procedures were performed in accordance with the approved protocols of

88 the Institutional Animal Care and Use Committee of the University of California, Davis, which
89 conforms to the Guide for the Care and Use of Laboratory Animals published by the US National
90 Institutes of Health (8th Edition, 2011). Mice were selected to undergo either sham-operation, or
91 ischemia followed by 24 hours [triphenyltetrazolium chloride (TTC) staining and cardiac troponin
92 measurements], 36 hours [in vivo imaging (IVIS) and fluorescence assisted cell sorting (FACS)
93 analysis], or 2 weeks (electrophysiology, histology, immunohistochemistry) of reperfusion (I/R).
94 Mice were anesthetised with 80 mg/kg ketamine and 5 mg/kg xylazine, intraperitoneal, prior to
95 surgery. After toe pinch and corneal reflexes were lost, ischemia was induced by ligating the
96 proximal LAD coronary artery for 45 minutes. Anaesthesia was maintained by supplementing 1%
97 isoflurane throughout the I/R procedure. Mice were injected with 100 µl of either 0.9% saline or
98 30 µM DS-IkL in saline via the tail vein immediately after reperfusion and at t=24 hours. Mice
99 were randomly selected to receive either DS-IkL or saline. Mice were given buprenorphine twice
100 daily for 48-72 hours post-operation (0.1 mg/kg subcutaneously). For euthanasia, mice were
101 injected with 80 mg/kg ketamine and 5 mg/kg xylazine to achieve a surgical plane of anaesthesia
102 followed by exsanguination upon removal of the heart. Cardiac structure and function, and
103 neutrophil and macrophage aggregation, were assessed 2 weeks after surgery. For the *in vivo*
104 imaging system and flow cytometry experiments, mice were allowed to recover for 36 hours after
105 surgery. Animals were imaged on an IVIS Spectrum in vivo imaging system (Perkin Elmer) under
106 1% isoflurane 1, 12, 24, and 36 hours after reperfusion prior to euthanasia. For TTC staining and
107 troponin analysis, mice were euthanized 24 hours following reperfusion.

108

109 **Peptide Library**

110 A combinatorial peptide library biased toward a known 7-mer selectin-binding peptide
111 sequence, Ile-Glu-Leu-Leu-Asp-Ala-Arg^{19, 20}, was created using the one-bead-one-peptide split
112 synthesis method²¹ on Tentagel S resin. The library was split a total of 7 times, yielding 31⁷ unique
113 sequences (**Figure 1**). Protecting groups were cleaved (82.5% trifluoroacetic acid, 5% phenol, 5%
114 water, 5% thioanisole, 2.5% triisopropylsilane) and resin screened for binding to recombinant
115 human E-selectin Fc chimera. One sequence, Ile-(D)Lys-Leu-Leu-(D)Pro-Hydroxyproline-Arg
116 (IkL) was selected for use in the experiments described herein.

117

118 **DS-IkL Synthesis**

119 Dermatan sulphate (DS, 41816 Da, Celsus Laboratories) was dissolved in phosphate buffer
120 (pH 4.54) and reacted with 45 equivalents of 4-(4,6-dimethoxy-1,3,5-triazin-2-yl)-4-methyl-
121 morpholinium chloride (DMTMM) for 5 minutes. HyNic-GRGsIkLLpHypR (IkL) (InnoPep) was
122 dissolved in phosphate buffer and added to the reaction. The reaction was left to complete for 48-
123 60 hours at room temperature with constant shaking, quenched with water, then filtered using
124 tangential flow filtration. Purified molecules were frozen and lyophilized for future use. The
125 number of peptides bound was quantified by reading absorbance at 280 nm on a NanoDrop
126 Microvolume Spectrophotometer (ThermoFisher Scientific) and comparing it to a standard curve
127 of free peptide. Unless otherwise stated, molecule with an average of 14-16 peptides bound per
128 DS was used for the present studies. For fluorescent molecules, CF594 Dye Hydrazide (Biotum)
129 was conjugated to DS using 2 equivalents of DMTMM and the complex purified before
130 conjugation to IkL.

131

132 **Cell Culture**

133 Human cardiac microvascular endothelial cells (HCMEC, PromoCell) p4-6 were used.
134 Stimulation media was prepared by diluting to 0.4 ng/ml tumour necrosis factor alpha (TNF- α)
135 and 0.3 ng/ml interleukin 1 beta (IL-1 β) in complete endothelial growth medium MV (PromoCell).
136

137 **Neutrophil and Platelet Isolation**

138 Human whole blood was collected into EDTA (neutrophil experiments) or sodium citrate
139 (platelet experiments) tubes in accordance with approved protocols of the Institutional Review
140 Board Administration at UC Davis, which conform to the principles outlined in the Declaration of
141 Helsinki. All participants gave informed consent prior to participation in the study. Neutrophils
142 were isolated using an EasyStep Direct Human Neutrophil Isolation Kit (Stem Cell Technologies)
143 and used at $0.3\text{-}2 \times 10^6$ cells/ml in Hank's Balanced Salt Solution with calcium and magnesium
144 (HBSS^{+/+}) supplemented with 0.1% human serum albumin (HSA). For HCMEC binding
145 experiments, neutrophils were stained with 1.5 nM Calcein-AM (BioLegend) for 30 minutes at
146 37°C before use. For microsphere experiments, neutrophils were stained with AF488 anti-human
147 CD11a/CD18 (clone m24) and PE anti-human CD15 (clone HI98) antibodies (BioLegend) for 20
148 minutes on ice. For platelet experiments, blood was separated by centrifugation for 20 minutes at
149 200xg; the resultant platelet rich plasma (PRP) layer was collected and used.

150

151 **Platelet Activation**

152 HCMECs were grown to confluence on 96-well CellBind plates then treated with 30 μ M
153 DS-IkL, 450 μ M IkL peptide, or 30 μ M DS in stimulation media for 4 hours. Wells were rinsed
154 2x with HBSS^{+/+} then treated with 100 μ L of PRP at 37°C. After 1 hour, 45 μ L of PRP was
155 removed from each well and added to tubes containing 5 μ L of ETP [107 mM

156 Ethylenediaminetetraacetic acid, disodium salt (EDTA), 12 mM Theophylline, and 2.8 μ M
157 Prostaglandin E1 in water]. Samples were briefly centrifuged and flash frozen.

158

159 **NAP-2 and PF-4 ELISA**

160 Unless otherwise stated, all incubations occurred at room temperature with shaking (700
161 RPM) and wells were rinsed 3x with PBS+0.05% Tween 20 (PBST) or 1% BSA in PBS between
162 steps. Mouse monoclonal anti-hNAP-2 IgG and anti-hPF4 IgG_{2B} capture antibodies (R&D
163 Systems) were coated on 96-well EIA/RIA high binding plates (Corning) at 2 μ g/mL in 1x PBS
164 and incubated at 4°C overnight. Wells were then blocked for 1 hour with 1% BSA. Samples were
165 thawed and centrifuged at 2000 x g for 20 minutes and supernatant diluted 1:5000 in 1% BSA.
166 Blocking buffer was removed (no rinse) and samples added for 2 hours. Biotinylated polyclonal
167 goat anti-hNAP-2 IgG and anti-hPF4 IgG detection antibodies (R&D systems) were added at 0.2
168 μ g/ml in 1% BSA for 2 hours. Streptavidin-HRP (diluted 1:200 in PBS) was then added for 20
169 minutes. Colorimetric change was induced with 1:1 hydrogen peroxide:tetramethylbenzidine
170 solution for 20 minutes. The reaction was stopped by addition of 2N sulfuric acid and absorbance
171 measured at 450 nm and 540 nm. Signals were subtracted to obtain a final absorbance.

172

173 **Neutrophil Binding to E-selectin Coated Microspheres**

174 Fluoresbrite 641 1.75 μ m carboxylate microspheres were coated with 10 μ g/ml E-selectin
175 using a PolyLink coupling kit (PolySciences, Inc.). Functionalized microspheres were treated with
176 HBSS^{+/+} (vehicle), EC-SEAL (30 μ M), DS-IkL₁₀ (30 μ M), or DS-IkL₁₅ (30 μ M) for one hour.
177 Microspheres were pelleted at 1000xg and resuspended in stained isolated human neutrophils, then
178 incubated for 30 minutes at room temperature with rotation. Samples were fixed in 4%

179 paraformaldehyde (PFA) and read on an Attune NxT Flow Cytometer (Invitrogen). Data was
180 analysed using FlowJo software.

181

182 **Neutrophil Binding to HCMECs**

183 HCMECs were grown to confluence in a tissue culture treated 96-well plate, stimulated for
184 4 hours, then treated with DS-IkL (30 μ M), DS (30 μ M), IkL alone (450 μ M), or HBSS^{+/+}
185 containing 0.2% HSA (vehicle) for 1 hour. Cells were washed twice with HBSS^{+/+} then treated
186 with 50,000 Calcein-AM labelled neutrophils per well with rotation (150 RPM, 37°C). After 30
187 minutes, cells were washed to remove non-adherent neutrophils and fluorescence read on a
188 SpectraMax M5 plate reader (Molecular Devices).

189

190 **CF594-DS-IkL Binding to Selectin Surfaces**

191 Piranha etched glass coverslips were coated with 0.2 mg/ml protein A/G and 25 mM
192 (bis(sulfosuccinimidyl)suberate) (BS3) overnight before being adhered to sticky-Slides VI 0.4-
193 untreated (Ibidi). Channels were coated with E-selectin-FC or P-selectin-FC at 20 μ g/ml (R&D
194 Systems) for 1.5 hours with rocking, blocked with 0.2% HSA for 1 hour, then treated with serially
195 diluted CF594-DS-IkL in HBSS^{+/+} for 1 hour with rocking. Channels were rinsed and stored in
196 HBSS^{+/+} at 4°C overnight before imaging to remove non-specifically bound molecule, then imaged
197 on a Nikon TE2000 inverted microscope (Nikon, Minato, Tokyo, Japan). For each channel, five
198 images were acquired in random locations and average fluorescence (mean grey value) within a
199 two-dimensional region of interest (ROI) quantified using ImageJ.

200

201 **Echocardiography**

202 Cardiac structure and function were monitored using 2D echocardiography (VisualSonic
203 Vevo 2100 with a MS 550D probe). All mice underwent echocardiography 2 weeks after either
204 sham-operation or I/R surgery. Systolic function was recorded under conscious conditions, while
205 diastolic function was recorded with isoflurane (~0.5-1%). Systolic function was acquired from 2-
206 D M-mode images and B-mode videos at the short axis, and diastolic function was obtained from
207 pulse-wave Doppler images.

208

209 **Fibrosis Measurements**

210 After 2 weeks, hearts from all four groups were fixed in 4% PFA solution in PBS, followed
211 by paraffin embedding. Five micrometre sections were cut at the transverse plane of the heart, at
212 the point of ligation. Sections were then deparaffinized in a series of xylene/alcohol (xylene,
213 xylene, 1:1 xylene:ethanol, 100% ethanol, 100% ethanol, 95% ethanol, 70% ethanol, 50% ethanol;
214 3 minutes in each solution). These sections were stained for both Picrosirius Red and Masson's
215 Trichrome, which provide information on the collagen level. Images were analysed in a blinded
216 fashion.

217

218 **Cell Isolation**

219 Cells were isolated using a Langendorff perfusion system as previously described²². After
220 isolation, cells were fixed in 0.4% PFA, and then subjected to flow cytometry.

221

222 **Flow Cytometric Analysis of Non-Myocyte Cells**

223 Single cell suspension was obtained from 10- to 12-week-old C57BL/6 mice as described
224 above. The cells were re-suspended in Ca²⁺ and Mg²⁺ free PBS, treated with phytoerythrin-

225 conjugated anti-Thy1.2 (BD Bioscience, San Diego, CA), anti-CD11b, anti-Ly-6C, anti-Ly-6G
226 (BD Bioscience), anti-CD31 (BD Bioscience), anti-MyHC (Developmental Studies Hybridoma
227 Bank, created by NICHD of the NIH and maintained at The University of Iowa, Department of
228 Biology, Iowa City, IA), and proliferation-specific Ki67 antibodies (BD Bioscience). Cells were
229 also stained with 40 µg/ml 7-amino- actinomycin D (7AAD, BD Bioscience, San Jose, CA) to
230 measure the DNA content. Data was collected using a standard FACScan cytometer (BD
231 Biosciences, San Jose, CA) upgraded to a dual laser system with the addition of a blue laser (15
232 mW at 488 nm) and a red laser (25 mW at 637 nm Cyttek Development, Inc, Fremont, CA) or
233 Becton Dickinson LSR-II Flow Cytometer. Data was acquired using CellQuest and DIVA 6.2
234 software (BD Bioscience). Cells stained with isotype-matched IgG antibodies were used as
235 controls to determine the positive cell population. Data was analysed using FlowJo software
236 (ver9.4 Treestar Inc., San Carlos).

237

238 **IVIS Imaging**

239 Mice were injected with 30 µM CF594-DS-IkL or free fluorophore in 0.9% saline after
240 surgery and after 24 hours (100 µl via the tail vein). Prior to imaging, mice were anesthetized by
241 isoflurane inhalation. Mice (n=6 per group) were imaged in an IVIS Spectrum Imaging System
242 (PerkinElmer). Fluorescent images were taken 1, 12, and 24 hours after the initial injection, and
243 12 hours after the second injection (36 hours after the initial injection). Images were analysed using
244 Living Image system software (PerkinElmer, version 4.3.1). Two-dimensional ROI circles were
245 drawn around the heart to quantify fluorescence and a control ROI was drawn on the flank to
246 quantify background. Fluorescence values were normalized to background by dividing average
247 radiant efficiency of heart by that of background.

248

249 **Immunohistochemistry (IHC)**

250 Hearts were fixed in 4% PFA overnight then washed with PBS the following day. Hearts
251 were paraffin embedded and sliced into 5 μ m sections. The sections were deparaffinized with
252 xylene and rehydrated in a descending grade of ethanol. Antigen retrieval was performed in Citrate
253 Buffer (pH 6.0, 15 mins at 95°C). Sections were permeabilized with 0.25% Triton X-100 in PBS
254 for 30 minutes at room temperature, and then blocked with 5% donkey serum diluted by 0.25%
255 Triton X-100. For macrophage staining, sections were incubated with rat anti-F4/80 (BioLegend,
256 monoclonal, 1:200) and mouse anti- α -Actinin (Sigma, monoclonal, 1:200) primary antibodies. For
257 neutrophil staining, primary antibodies used were rat anti-Ly6G (BioLegend, monoclonal, 1:200)
258 and mouse anti- α -Actinin (Sigma, monoclonal, 1:200). Primary antibodies were diluted in
259 blocking solution and sections incubated overnight at 4°C. Secondary antibodies used were donkey
260 anti-mouse Alexa Fluor 488 (Invitrogen, 1:500) or donkey anti-rat Alexa Fluor 554 (Abcam,
261 1:500). Secondary antibodies were diluted in blocking solution and incubated for 1 hour at room
262 temperature. Slides were mounted and then imaged using a Zeiss confocal LSM 700 microscope.
263 Images were analysed by ImageJ.

264

265 **TTC Staining**

266 Hearts were embedded in 2% agarose gel in a heart matrix, then subsequently sliced into
267 1-1.5 mm sections. Sections were immersed in 1% TTC solution for 30 mins at 37°C. They were
268 then fixed in 4% PFA for 20 minutes before images were taken under a dissection microscope
269 connected to a Dino-Lite USB microscope.

270

271 **Troponin I Measurements**

272 Troponin I (CNTI) was measured using a commercial kit (Life Diagnostics) according to
273 the manufacturer instructions. Sample concentrations were calculated from a standard curve
274 generated in GraphPad Prism (San Diego, CA) using 4-parameter logistic regression. Sample
275 concentrations were multiplied by their respective dilution factors to obtain final concentration
276 values.

277

278 **Statistics**

279 All *in vitro* experiments were repeated at least 3 times for an $n \geq 3$. Each experiment was
280 performed with 3-4 technical replicates. Data were analysed using one-way or two-way ANOVA
281 with post-hoc Tukey multi-comparisons analysis. Data are represented as means \pm SEM.

282

283 **RESULTS**

284 ***Combinatorial peptide library screening generated the selectin-binding sequence, IkLLpHypR***

285 Selectins mediate the initial capture of leukocytes to the vascular surface¹⁶ and are therefore
286 a promising target for modulating leukocyte recruitment. We first set out to create a combinatorial
287 peptide library containing unnatural amino acids, biased toward the selectin binding sequence of
288 EC-SEAL, a molecule we previously described^{19, 20}. We used the one-bead-one-compound
289 combinatorial library method, which allows for the unrestricted incorporation of natural and
290 unnatural amino acids (**Figure 1**)²¹, to discover the sequence Ile-(D)Lys-Leu-Leu-(D)Pro-
291 Hydroxyproline-Arg.

292

293 *DS-IkL exhibited binding to E- and P-selectin coated surfaces and reduced neutrophil binding*
294 *to E-selectin in solution*

295 To confirm that DS-IkL binds selectins, P- and E-selectin coated surfaces were treated with
296 increasing concentrations of DS-IkL or DS alone. Dermatan sulphate (DS) is a negatively charged
297 proteoglycan that is known to interact with P-selectin²³. We directly determined if the addition of
298 IkL would improve binding to P- or E-selectin compared to DS alone. **Figure 2** shows that DS-
299 IkL exhibited significantly enhanced binding to both selectins with increasing concentrations of
300 molecule, which is not observed in the DS group. The ability of DS-IkL to interfere with E-selectin
301 binding to neutrophils in suspension was further confirmed in **Supplementary Figure 1**.
302 Treatment with DS-IkL inhibited neutrophil binding to E-selectin, but not P-selectin, at 5-30 μM
303 concentrations by up to 35%. These reductions were similar to those seen on endothelial cell
304 surfaces (**Figure 3D**). Higher concentrations were needed to reduce P-selectin binding. Similarly,
305 in the presence of DS-IkL, stimulated neutrophils bound less E-selectin, but not intercellular
306 adhesion molecule-1 (ICAM-1) (**Supplementary Figure 1**), suggesting DS-IkL preferentially
307 binds E-selectin.

308

309 *Treatment with DS-IkL significantly reduced platelet activation on stimulated endothelial cells*

310 Enhanced platelet activation and binding have been implicated in a multitude of chronic
311 inflammatory diseases, including acute coronary and pulmonary syndromes²⁴. Activated platelets
312 release cytokines such as platelet factor 4 (PF-4) and neutrophil activating peptide 2 (NAP-2) that
313 can in turn activate neutrophils²⁵. Given their contributions to neutrophil recruitment to sites of
314 inflammation, we aimed to test if treatment of inflamed ECs with DS-IkL could reduce PF-4 and
315 NAP-2 activation of platelets. Platelets were allowed to interact with stimulated HCMECs under

316 standard culture conditions for 1 hour before supernatant was collected. Levels of PF-4 and NAP-
317 2 that accumulated in the supernatant during this time were significantly diminished in DS-IkL
318 treated cells ($p < 0.05$), as shown in **Figure 3A-B**. Notably, DS-IkL reduced NAP-2 activation on
319 stimulated HCMECs to levels similar to unstimulated controls, implying our molecule has the
320 potential to act as a barrier to platelet-induced neutrophil activation.

321

322 *DS-IkL reduced neutrophil arrest on E-selectin coated microspheres and stimulated endothelial*
323 *cells*

324 The neutrophil adhesion cascade begins with initial capture and slow rolling along selectins
325 that are upregulated on inflamed endothelium and activated platelets; therefore, interfering with
326 this initial capture could prove therapeutically beneficial. To test our molecule's ability to block
327 neutrophil-selectin interactions, E-selectin coated microspheres were treated with DS (30 μM),
328 IkL peptide (450 μM), DS-IkL (30 μM), DS-IkL₁₀ (30 μM), or vehicle prior to incubation with
329 isolated human neutrophils. Only IkL peptide and DS-IkL were able to reduce neutrophil adhesion
330 to microspheres to approximately 75% of control ($p < 0.05$, **Figure 3C**), with DS and DS-IkL₁₀
331 exhibiting similar neutrophil-microsphere colocalization as control. Given the importance of
332 tightly regulated neutrophil capture and activation in proper wound healing²⁶, this slight reduction
333 could be the tipping point back toward a restorative state.

334 We next sought to investigate if the effect of DS-IkL on neutrophil-selectin interactions
335 was retained on ECs, which are known to upregulate their selectin expression upon stimulation
336 with inflammatory cytokines such as TNF- α and IL-1 β ²⁷. HCMECs were treated with DS-IkL
337 under stimulatory conditions prior to incubation with neutrophils. Neutrophils exhibited reduced
338 adhesion to treated ECs as compared with vehicle controls ($p < 0.01$, **Figure 3D**), to a similar extent

339 as on selectin-coated microbeads. These results support our hypothesis that DS-IkL reduces
340 selectin-mediated neutrophil capture at sites of inflammation.

341

342 *DS-IkL targeted to the heart after I/R*

343 Since DS-IkL suppressed neutrophil adhesion *in vitro*, we investigated whether this would
344 occur *in vivo* following a myocardial infarction, induced by 45 minutes of ischemia at the LAD
345 with subsequent reperfusion. To verify proper occlusion of the LAD, we monitored ECG
346 recordings during occlusion (**Supplementary Figure 1**). Only I/R mice with ST-segment
347 elevations were included in the I/R group. Immediately after sham or LAD operation, we injected
348 either 30 μ M DS-IkL conjugated to a fluorophore (CF594-DS-IkL) or saline with equal
349 concentration of the fluorophore, and monitored *in vivo* fluorescent intensity at 1, 12, 24, and 36
350 hours after surgery. Representative images of all four groups are shown in **Figure 4A**. As
351 evidenced by these images, fluorescence signals were primarily localized to the cardiac region
352 only in the I/R group after the CF594-DS-IkL injection. We observed some targeting to throat
353 regions that sustained damage during tracheotomy, as well as background fluorescence in the
354 abdomen, likely from autofluorescent components of mouse chow²⁸. Quantitatively, signal
355 intensity was significantly higher an hour after surgery in mice treated with DS-IkL after I/R,
356 relative to mice treated with the fluorophore dissolved in saline ($p < 0.001$, **Figure 4B**). There was
357 no difference in fluorescent intensity in the cardiac region in saline sham mice vs saline I/R mice,
358 suggesting that the molecule just circulated in the blood, but did not localize to the heart. In
359 addition, fluorescent signal persisted for at least 24 hours in the cardiac region after I/R surgery in
360 mice treated with DS-IkL. After a subsequent dosage at the 24-hour mark, no noticeable difference
361 was observed in this group relative to the other groups at the 36-hour time point. Taken together,

362 our *in vivo* imaging suggested that DS-IkL targeted to the heart, and the binding of DS-IkL lasted
363 for at least 24 hours.

364

365 ***Mice treated with DS-IkL exhibited reduced infarct size and improved cardiac function after***
366 ***I/R***

367 To examine the *in vivo* effects of DS-IkL on cardiac structure and function, we performed
368 either sham or 45 mins I/R. To assess the short-term effects of DS-IkL on cardiac injury, we
369 administered one injection of either saline or DS-IkL immediately after surgery and examined the
370 degree of myocardial infarction and extent of cardiac injury after 24 hours of reperfusion.
371 Representative sections stained with TTC are displayed in **Figure 5A**. As evident from the
372 sections, I/R induced a more pronounced increase in damaged, non-viable cardiac regions, relative
373 to DS-IkL treated mice. Sham-operated sections are displayed in **Supplementary Figure 4**.
374 Quantification, percentage of infarcted region relative to left ventricular area, demonstrated a
375 significant reduction in infarct size in DS-IkL hearts (**Figure 5B**). Cardiac injury was assessed by
376 measuring cardiac Troponin I. Although there was not a significant difference, there was a trend
377 towards a reduction in injury at 24 hours post injury (**Figure 5C**).

378 To determine the long-term effects of DS-IkL, we performed the same procedure, but mice
379 were subjected to 2 weeks of reperfusion. To ensure robust activity of DS-IkL, we administered
380 an additional dose of DS-IkL 24 hours after surgery on top of the dose given immediately after
381 surgery. Cardiac structure and function were assessed 2 weeks post-operation. Representative M-
382 mode tracings at the parasternal short-axis are shown for all four groups and display the beat-to-
383 beat changes in wall thickness and diameter of the left ventricle (**Figure 5D**). Recordings were
384 performed in conscious mice; heart rate in all groups were therefore similar (**Figure 5E**).

385 Structurally, I/R resulted in an increase in the left ventricular mass in groups treated with either
386 saline or DS-IkL, relative to their respective sham-operated groups ($p < 0.05$, **Figure 5F**). Similar
387 to our echocardiography findings, I/R induced an increase in heart weight to tibial length ratio in
388 mice treated with either saline or DS-IkL, relative to their sham-operated controls
389 (**Supplementary Figure 2**). Even though I/R resulted in a reduction in fractional shortening
390 (**Figure 5G**) and ejection fraction (**Supplementary Table 1**) in both groups, there was a
391 significant improvement in fractional shortening in the DS-IkL treated mice compared to saline
392 alone ($p < 0.05$, **Figure 5G**). Furthermore, strain analysis revealed a significant reduction in global
393 radial strain (**Figure 5H**) in both I/R groups relative to their respective sham groups. However, the
394 decrease was significantly less in DS-IkL mice treated groups. Although the local radial strain was
395 not significant (**Figure 5I**), the small improvement in all the different regions of the heart
396 contributed to an overall and global increase in global radial strain in DS-IkL mice. Global
397 circumferential strain was significantly reduced in saline treated mice relative to their control sham
398 (**Figure 5J**). However, this was not observed in DS-IkL treated mice.

399 Diastolic function was assessed using the blood flow velocity through the mitral valve
400 during the cardiac cycle. Representative tracings using pulse-wave Doppler show two distinct
401 waveforms, which correspond to left ventricular filling during early diastole (E wave) and left
402 ventricular filling during late diastole (A wave, **Figure 5K**). The ratio of the two provides an
403 indication of diastolic function²⁹. Mice treated with DS-IkL did not exhibit a change in diastolic
404 function, as compared to their sham control; whereas, mice treated with saline showed a significant
405 reduction in the E/A ratio, indicating an impairment in diastolic function (**Figure 5L**). Indeed, the
406 E/A ratio of mice treated with DS-IkL was significantly higher than mice treated with saline, after
407 I/R ($p < 0.05$). Although the isovolumetric relaxation time (IVRT, **Figure 5M**) did not change

408 significantly, the MV deceleration time was significantly elevated in the I/R group treated with
409 saline, relative to the saline sham group ($p < 0.05$, **Figure 5N**). This was not seen when the mice
410 were treated with DS-IkL. Together, these data suggest that both systolic and diastolic function
411 was significantly improved with the treatment with DS-IkL.

412

413 *DS-IkL limited fibrosis after I/R*

414 MI induces loss of cardiomyocytes with concomitant increase in fibrosis³⁰. Histological
415 analyses of cardiac sections were performed 2 weeks after I/R. Representative whole heart images
416 of all four groups, and short-axis sections stained with Masson's Trichrome (MT) and Picrosirius
417 Red (PSR) are shown (**Figure 6A**). Percentages of fibrotic area relative to the total left ventricular
418 area were quantified in a blinded fashion and were low and not significantly different in the sham-
419 operated groups. In contrast, there was a significant elevation in collagen deposition in both I/R
420 groups, relative to their respective sham-operated controls ($p < 0.01$, **Figure 6B**). However, I/R
421 mice treated with DS-IkL showed significantly less fibrosis than mice treated with saline (**Figure**
422 **6D-E**, $p < 0.05$), consistent with TTC data observed 24 hours after I/R (**Figure 5A-B**). Together,
423 the data show that DS-IkL limited fibrosis, which in part contributed to the improved cardiac
424 function as assessed by echocardiography.

425

426 *DS-IkL prevented neutrophil and macrophage aggregation, fibroblast proliferation, and* 427 *endothelial cell proliferation after I/R*

428 I/R causes cardiac endothelial cell dysfunction, leading to an amplified inflammatory state
429 and an increase in vascular permeability³¹. If not tightly regulated, immune cells recruited to the
430 damaged regions accentuate damage and contribute to tissue fibrosis. To determine the effect of

431 DS-IkL on neutrophil and fibroblast accumulation, we isolated non-myocyte cell populations from
432 the hearts from all four groups 36 hours after sham or I/R surgeries. Flow cytometric analysis
433 showed a significant increase in CD11b⁺/Ly6-C/G⁺ neutrophils in the saline treated I/R group
434 compared to sham controls (p<0.05), but no significant increase in the DS-IkL treated I/R group
435 (**Figures 7A-B**), suggesting that treatment with DS-IkL limited neutrophil accumulation after I/R.
436 Furthermore, there was a significant increase in both total (CD31⁺) and proliferative ECs
437 (Ki67⁺/CD31⁺) in the saline I/R group, but not in the DS-IkL treated I/R groups (**Figures 7C-E**),
438 suggesting a significant decrease in adverse vascular remodelling by DS-IkL. Moreover, the
439 percentage of proliferative fibroblasts (Thy1.2⁺) in the saline I/R group was significantly higher
440 than in the DS-IkL treated I/R group (**Figures 7F-H**), consistent with the significant increase in
441 collagen deposition observed 2 weeks after reperfusion. It must be noted that CD45 was not used
442 to gate out hematopoietic cells that may also be positive for CD31 or Thy1.2. Thus, while the
443 changes in endothelial and fibroblast cell numbers are suggestive, future work is needed to
444 definitively show these changes.

445 Although the immune response is heightened shortly after MI, the effects can manifest
446 long-term as the body tries to re-establish homeostasis. To determine the long-term effects of DS-
447 IkL on neutrophil and macrophage accumulation, we performed immunohistochemistry on all four
448 groups after 2 weeks of I/R. Representative images of IHC are shown in **Figure 7I**. Tissue sections
449 were stained with α -actinin to stain for cardiomyocytes, F4/80 to stain for macrophages, and Ly6G
450 to stain for neutrophils. DS-IkL treatment significantly reduced the number of macrophages per
451 area (**Figures 7I and 7J**) and neutrophils per area (**Figures 7I and 7K**) at both 36 hours (Figure
452 7I) and 2 week (Figures 7J and 7K). Together, our data suggest that DS-IkL limited neutrophil and
453 macrophage aggregation, as well as fibroblast and EC proliferation. Mechanistically, DS-IkL

454 treatment prevented multiple aspects of the immune response by acting as a molecular bandage on
455 the damaged endothelial surface, which ultimately resulted in less fibrosis and improved cardiac
456 function (**Figure 7L**).

457

458

DISCUSSION

459 Inflammatory responses significantly contribute to further injury after the initial insult of
460 an MI. Ischemic coronary vessels undergo drastic alterations to their microstructure and
461 homeostasis upon reperfusion, conducive to immune cell infiltration. Ion imbalance disrupts cell-
462 cell junction integrity along the endothelium³², creating migration points for neutrophils and
463 macrophages that are recruited to these cytokine-rich environments³¹. Furthermore, ECs exhibit
464 signs of endothelial cell dysfunction, namely enhanced cell contractility, upregulated cell adhesion
465 molecules such as E- and P-selectin, and the loss of the glycocalyx^{10, 31}. The dysfunctional EC
466 phenotype facilitates neutrophil recruitment and extravasation. Neutrophils that have been
467 recruited to these sites activate and secrete a milieu of pro-inflammatory cytokines that in turn
468 recruit additional leukocytes³³, shifting the inflammatory process from restorative to destructive.
469 Therapeutics that limit the initial binding and activation of circulating immune cells could tip the
470 balance back to a restorative state.

471

472 **Design of the novel DS-IkL**

473 We previously described a molecule termed “EC-SEAL” composed of oxidized dermatan
474 sulphate (DS), to which known selectin-binding peptides were conjugated via a heterobifunctional
475 crosslinker¹⁹. Although EC-SEAL mitigated the immune response *in vitro*, it is not an acceptable
476 drug candidate for the clinic. The chemistry used to functionalize the DS uses glycol splitting by

477 periodate oxidation, a mechanism which cleaves carbohydrate rings at vicinal diols to create a
478 reactive intermediate³⁴. This chemistry renders the molecule unstable; thus, it cannot be stored
479 long-term. Furthermore, the chain conformation changes dramatically, resulting in a chain coiled
480 polymer chain rather than an extended linear structure seen with natural glycosaminoglycans.

481 In this study, we designed an improved molecule termed DS-IkL. We demonstrated that
482 DS could be modified with peptides without cleaving the ring structure and still maintain the ability
483 to bind to the selectin receptors to interfere with platelet and neutrophil binding. Importantly, this
484 new chemistry, which better maintains DS structure, eliminates the reactive intermediates that
485 reduced the stability of EC-SEAL. Additionally, the selectin binding sequence in EC-SEAL
486 consisted solely of L-amino acids, which are readily degraded by proteolytic enzymes present at
487 sites of inflammation. Though not directly addressed here, we believe that the incorporation of D-
488 amino acids within the selectin binding sequence delays DS-IkL's degradation and clearance,
489 supporting its presence on ECs for at least 24 hours.

490 To design DS-IkL, we first created a combinatorial peptide library containing unnatural
491 amino acids, biased toward the E-selectin binding sequence of EC-SEAL^{19,20}. We chose to use the
492 one-bead-one-compound combinatorial library method, which allows for the unrestricted
493 incorporation of natural and unnatural amino acids²¹, to discover the sequence I-k-L-L-p-Hyp-R.
494 Our preliminary efforts focused on the ability of IkL peptide and our DS-IkL glycoconjugate to
495 bind selectins (**Figure 2**) and interfere with neutrophil binding to E-selectin coated microspheres
496 (**Figure 3A**). Selectins mediate the initial capture of leukocytes to the vascular surface¹⁶, and are
497 therefore a promising target for modulating leukocyte recruitment. We hypothesized that selectins
498 blanketed with our glycoconjugate would be masked from circulating leukocytes, therefore
499 limiting their capture. In line with this hypothesis, we observed significant reductions in neutrophil

500 binding to both selectin coated microspheres and stimulated ECs upon treatment with DS-IkL₁₅,
501 suggesting DS-IkL₁₅ interacted with upregulated selectins on the cell surface.

502

503 **DS-IkL reduced platelet activation on endothelial cells**

504 Given the destructive role platelets play in myocardial I/R injury^{17, 35}, we were interested
505 in DS-IkL's effect on the activation state of platelets incubated on stimulated ECs. Interestingly,
506 we saw significant reductions in NAP-2 levels and a trend toward reduction in PF-4 in cultures
507 that had been pre-treated with DS-IkL as compared to HBSS treated controls, suggesting ECs
508 treated with DS-IkL presented fewer available platelet activating ligands such as endothelial P-
509 selectin. Though we did not observe significant reductions in PF-4, a chemokine which induces
510 firm adhesion of neutrophils in the presence of TNF- α ^{25, 36}, we believe our modest results may be
511 an artefact of the experiment. PF-4 has an affinity for GAGs³⁶ and therefore may have been
512 sequestered by DS-IkL or heparin on the cell surface or within the media.

513 In addition to direct damage caused by activated platelets, these bioactive blood
514 components have been shown to play a pivotal role in neutrophil capture along inflamed
515 endothelium, offering an anchor point via platelet P-selectin and facilitating endothelial
516 transmigration^{24, 35}. Although E- and P-selectin are very similar molecules, both in structure and
517 function, we observed slight differences in binding to E- and P-selectin coated surfaces (**Figure**
518 **2**), with DS-IkL exhibiting more consistent binding to E-selectin at higher concentrations. Our
519 results suggest that IkL peptide plays a more influential role in E- and P-selectin binding when
520 DS-IkL is administered at higher concentrations, whereas at lower concentrations, selectin binding
521 may be influenced more by DS. By interacting with both P- and E-selectin, DS-IkL may
522 simultaneously protect from neutrophil interactions, platelet aggregation, and the formation of

523 platelet-neutrophil complexes. Therefore, DS-IkL presents a two-fold cardioprotective potential
524 by limiting damage from both activated platelets and neutrophils.

525

526 **DS-IkL improved cardiac function by disrupting components of the immune response**

527 Since one of the hallmarks of reperfusion injury is overactivation of the immune system
528 due to leukocyte accumulation and platelet activation, we assessed the potential therapeutic
529 benefits of DS-IkL in a clinically relevant murine model of I/R. Our data show that DS-IkL
530 localized to the damaged cardiac region (**Figure 4**) and limited neutrophil and fibroblast
531 accumulation after I/R, which resulted in less tissue fibrosis (**Figure 6**), reduced myocardial
532 infarction, and improved cardiac function (**Figure 5**). Interestingly, DS-IkL treated I/R mice did
533 not exhibit the increase in total and proliferative ECs that was observed in the saline I/R group. In
534 some cases, a heightened presence of proliferative ECs may indicate tissue regeneration³⁷;
535 however, the saline treated I/R group exhibited poor cardiac function and enhanced fibrosis. Our
536 results therefore suggest that rather than regeneration, early remodelling and myocardial
537 hypertrophy was beginning to occur, necessitating an increase in cardiac angiogenesis³⁸.

538

539 **Proposed Mechanism of DS-IkL**

540 Other attempts have been made to limit I/R induced injury after MI³⁹, including ischemic
541 pre- and postconditioning, pharmacologic interventions targeting metabolic pathways that
542 contribute to RI^{40, 41}, and the use of monoclonal antibodies to limit platelet and neutrophil
543 adhesion³⁹. In particular, antibody therapy to P-selectin^{42, 43} and ICAM-1 have been investigated
544 as cardioprotective therapies against neutrophil and platelet mediated RI⁴⁴. However, as evidenced
545 by the SELECT-ACS trial evaluating the effect of Inclacumab⁴⁵, a recombinant monoclonal

546 antibody against P-selectin, a major drawback of antibody therapy is the need for high doses for
547 therapeutic effect⁴⁶, lending to high production costs⁴⁷. It is worth noting that monoclonal P-
548 selectin antibody crizanlumab⁴⁸ (awarded Breakthrough Therapy designation) and the pan-
549 selectin inhibitor Rivipansel⁴⁹ (failed at Phase 3) have shown promise in vaso-occlusive crises in
550 sickle cell disease. However, neither of these have been tested in RI.

551 Our strategy is unique from antibody therapeutics. DS-IkL is generally smaller than
552 antibody therapeutics (~62 kDa) and has been designed to interrupt multiple parts of the immune
553 pathway simultaneously by masking adhesion molecules on the endothelial surface. We designed
554 a *molecular bandage* that targets DS – a native component of the glycocalyx – to inflamed
555 endothelium. By blanketing DS over the dysfunctional endothelial surface, we aimed to directly
556 reduce selectin availability while indirectly interfering with immune cell interactions with other
557 adhesion molecules on the endothelial surface. We demonstrated that DS-IkL binds to E- and P-
558 selectin, limited neutrophil and platelet adhesion to inflamed ECs, reduced neutrophil,
559 macrophage, and fibroblast accumulation after MI (**Figure 7**), and improved cardiac function after
560 MI. We conducted our current study at a treatment concentration of 30 μ M. **Figure 2** suggests DS-
561 IkL may have a greater therapeutic benefit at higher concentrations; therefore, future studies will
562 be required to determine the concentration of DS-IkL that produces the optimum therapeutic effect,
563 as well as to further elucidate the mechanism by which DS-IkL works.

564

565 **Conclusions**

566 We created DS-IkL using the one-bead-one-peptide synthesis approach. *In vitro*, DS-IkL
567 bound to both P- and E-selectin coated surfaces and prevented neutrophil binding and platelet
568 activation. *In vivo*, DS-IkL localized to the cardiac region in mice after MI and limited neutrophil

569 and fibroblast accumulation. Mice treated with DS-IkL exhibited improved cardiac function and
570 less fibrosis. Taken together, our data suggest that our recently developed, novel DS-IkL molecule
571 reduced the inflammatory response induced by MI, which resulted in cardioprotection.

572

573 **Acknowledgements**

574 This work was supported by a Predoctoral Fellowship from Tobacco-Related Disease Research
575 Program (TRDRP) T29DT0237 (TD), Postdoctoral Fellowships from NIH T32 Training Grant in
576 Basic & Translational Cardiovascular Science HL86350 and NIH F32 HL149288 (PNT), NIH R01
577 HL085727, HL085844, HL137228, and S10 RR033106, Research Award from the Rosenfeld
578 Foundation, VA Merit Review Grant I01 BX000576 and I01 CX001490 (NC). NC is the holder
579 of the Roger Tatarian Endowed Professorship in Cardiovascular Medicine and a part-time staff
580 physician at VA Northern California Health Care System, Mather, CA. The authors would like to
581 thank the Combinatorial Chemistry and Chemical Biology Shared Resource at University of
582 California Davis for assistance of synthesis and sequence decoding of OBOC peptide library.
583 Utilization of this Shared Resource was supported by the UC Davis Comprehensive Cancer Center
584 Support Grant awarded by the National Cancer Institute (NCI P30CA093373).

585

586 **Authors' Contributions**

587 TD and PNT designed the research study, conducted experiments, acquired data, analysed data,
588 and wrote the manuscript. HS, LR, and PS conducted experiments, acquired data, analysed data.
589 CN and VT conducted experiments. JLO analysed data. XL and KL helped conceptualize and
590 design the peptide library. NC and AP designed the research study, provided monetary support,
591 and wrote the manuscript.

592

593 **Data Availability Statement**

594 The data underlying this article are available in the Dryad Digital Repository,

595 <https://doi.org/10.25338/B8M32V>.

596

597 **Conflict of Interest**

598 The authors claim no conflict of interest.

599 **References**

600 1. Fryar CD, Chen TC, Li X. Prevalence of uncontrolled risk factors for cardiovascular
601 disease: United States, 1999-2010. *NCHS Data Brief* 2012;1-8.

602 2. Myerburg RJ, Junttila MJ. Sudden cardiac death caused by coronary heart disease.
603 *Circulation* 2012;**125**:1043-1052.

604 3. Kalogeris T, Baines CP, Krenz M, Korthuis RJ. Cell biology of ischemia/reperfusion injury.
605 *Int Rev Cell Mol Biol* 2012;**298**:229-317.

606 4. Hausenloy DJ, Yellon DM. Myocardial ischemia-reperfusion injury: a neglected
607 therapeutic target. *J Clin Invest* 2013;**123**:92-100.

608 5. Rusinkevich V, Huang Y, Chen Z-y, Qiang W, Wang Y-g, Shi Y-f, Yang H-t. Temporal
609 dynamics of immune response following prolonged myocardial ischemia/reperfusion
610 with and without cyclosporine A. *Acta Pharmacologica Sinica* 2019;**40**:1168-1183.

611 6. Frangogiannis NG. The inflammatory response in myocardial injury, repair, and
612 remodelling. *Nat Rev Cardiol* 2014;**11**:255-265.

613 7. Hausenloy DJ, Chilian W, Crea F, Davidson SM, Ferdinandy P, Garcia-Dorado D, van
614 Royen N, Schulz R, Heusch G. The coronary circulation in acute myocardial
615 ischaemia/reperfusion injury: a target for cardioprotection. *Cardiovasc Res*
616 2019;**115**:1143-1155.

617 8. Chappell D, Hofmann-Kiefer K, Jacob M, Rehm M, Briegel J, Welsch U, Conzen P, Becker
618 BF. TNF-alpha induced shedding of the endothelial glycocalyx is prevented by
619 hydrocortisone and antithrombin. *Basic Res Cardiol* 2009;**104**:78-89.

620 9. Mulivor AW, Lipowsky HH. Inflammation- and ischemia-induced shedding of venular
621 glycocalyx. *American Journal of Physiology-Heart and Circulatory Physiology*
622 2004;**286**:H1672-H1680.

623 10. McDonald KK, Cooper S, Danielzak L, Leask RL. Glycocalyx Degradation Induces a
624 Proinflammatory Phenotype and Increased Leukocyte Adhesion in Cultured Endothelial
625 Cells under Flow. *PLoS One* 2016;**11**:e0167576.

626 11. van Haaren PM, VanBavel E, Vink H, Spaan JA. Localization of the permeability barrier to
627 solutes in isolated arteries by confocal microscopy. *Am J Physiol Heart Circ Physiol*
628 2003;**285**:H2848-2856.

629 12. Sieve I, Munster-Kuhnel AK, Hilfiker-Kleiner D. Regulation and function of endothelial
630 glycocalyx layer in vascular diseases. *Vascul Pharmacol* 2018;**100**:26-33.

631 13. McDonald KK, Cooper S, Danielzak L, Leask RL. Glycocalyx degradation induces a
632 proinflammatory phenotype and increased leukocyte adhesion in cultured endothelial
633 cells under flow. *PLoS ONE* 2016;**11**.

634 14. Rehm M, Bruegger D, Christ F, Conzen P, Thiel M, Jacob M, Chappell D, Stoeckelhuber
635 M, Welsch U, Reichart B, Peter K, Becker BF. Shedding of the endothelial glycocalyx in
636 patients undergoing major vascular surgery with global and regional ischemia.
637 *Circulation* 2007;**116**:1896-1906.

638 15. Potter DR, Jiang J, Damiano ER. The recovery time course of the endothelial cell
639 glycocalyx in vivo and its implications in vitro. *Circ Res* 2009;**104**:1318-1325.

640 16. McEver RP. Selectins: initiators of leucocyte adhesion and signalling at the vascular wall.
641 *Cardiovasc Res* 2015;**107**:331-339.

- 642 17. Palazzo AJ, Jones SP, Anderson DC, Granger DN, Lefer DJ. Coronary endothelial P-
643 selectin in pathogenesis of myocardial ischemia-reperfusion injury. *Am J Physiol*
644 1998;**275**:H1865-1872.
- 645 18. Manchanda K, Kolarova H, Kerkenpaß C, Mollenhauer M, Vitecek J, Rudolph V, Kubala L,
646 Baldus S, Adam M, Klinke A. MPO (myeloperoxidase) reduces endothelial glycocalyx
647 thickness dependent on its cationic charge. *Arteriosclerosis, Thrombosis, and Vascular*
648 *Biology* 2018;**38**:1859-1867.
- 649 19. Wodicka JR, Chambers AM, Sangha GS, Goergen CJ, Panitch A. Development of a
650 Glycosaminoglycan Derived, Selectin Targeting Anti-Adhesive Coating to Treat
651 Endothelial Cell Dysfunction. *Pharmaceuticals (Basel)* 2017;**10**.
- 652 20. Wodicka JR, Morikis VA, Dehghani T, Simon SI, Panitch A. Selectin-Targeting Peptide-
653 Glycosaminoglycan Conjugates Modulate Neutrophil-Endothelial Interactions. *Cell Mol*
654 *Bioeng* 2019;**12**:121-130.
- 655 21. Lam KS, Lehman AL, Song A, Doan N, Enstrom AM, Maxwell J, Liu R. Synthesis and
656 screening of "one-bead one-compound" combinatorial peptide libraries. *Methods*
657 *Enzymol* 2003;**369**:298-322.
- 658 22. Timofeyev V, Myers RE, Kim HJ, Woltz RL, Sirish P, Heiserman JP, Li N, Singapuri A, Tang
659 T, Yarov-Yarovoy V, Yamoah EN, Hammond HK, Chiamvimonvat N. Adenylyl cyclase
660 subtype-specific compartmentalization: differential regulation of L-type Ca²⁺ current in
661 ventricular myocytes. *Circ Res* 2013;**112**:1567-1576.
- 662 23. Kawashima H, Hirose M, Hirose J, Nagakubo D, Plaas AH, Miyasaka M. Binding of a large
663 chondroitin sulfate/dermatan sulfate proteoglycan, versican, to L-selectin, P-selectin,
664 and CD44. *J Biol Chem* 2000;**275**:35448-35456.
- 665 24. Lisman T. Platelet-neutrophil interactions as drivers of inflammatory and thrombotic
666 disease. *Cell Tissue Res* 2018;**371**:567-576.
- 667 25. Pitchford S, Pan D, Welch HC. Platelets in neutrophil recruitment to sites of
668 inflammation. *Curr Opin Hematol* 2017;**24**:23-31.
- 669 26. Wang J. Neutrophils in tissue injury and repair. *Cell Tissue Res* 2018;**371**:531-539.
- 670 27. Kuldo JM, Westra J, Asgeirsdottir SA, Kok RJ, Oosterhuis K, Rots MG, Schouten JP,
671 Limburg PC, Molema G. Differential effects of NF- κ B and p38 MAPK inhibitors and
672 combinations thereof on TNF- α - and IL-1 β -induced proinflammatory status of
673 endothelial cells in vitro. *Am J Physiol Cell Physiol* 2005;**289**:C1229-1239.
- 674 28. Bhaumik S, DePuy J, Klimash J. Strategies to minimize background autofluorescence in
675 live mice during noninvasive fluorescence optical imaging. *Lab Animal* 2007;**36**:40-43.
- 676 29. Gao S, Ho D, Vatner DE, Vatner SF. Echocardiography in Mice. *Curr Protoc Mouse Biol*
677 2011;**1**:71-83.
- 678 30. Talman V, Ruskoaho H. Cardiac fibrosis in myocardial infarction-from repair and
679 remodeling to regeneration. *Cell Tissue Res* 2016;**365**:563-581.
- 680 31. Yang Q, He GW, Underwood MJ, Yu CM. Cellular and molecular mechanisms of
681 endothelial ischemia/reperfusion injury: perspectives and implications for postischemic
682 myocardial protection. *Am J Transl Res* 2016;**8**:765-777.
- 683 32. Li W, Wang W. Structural alteration of the endothelial glycocalyx: contribution of the
684 actin cytoskeleton. *Biomechanics and modeling in mechanobiology* 2018;**17**:147-158.

- 685 33. Ley K, Laudanna C, Cybulsky MI, Nourshargh S. Getting to the site of inflammation: the
686 leukocyte adhesion cascade updated. *Nat Rev Immunol* 2007;**7**:678-689.
- 687 34. Perlin AS. Glycol-cleavage oxidation. *Adv Carbohydr Chem Biochem* 2006;**60**:183-250.
- 688 35. Xu Y, Huo Y, Toufektsian MC, Ramos SI, Ma Y, Tejani AD, French BA, Yang Z. Activated
689 platelets contribute importantly to myocardial reperfusion injury. *Am J Physiol Heart*
690 *Circ Physiol* 2006;**290**:H692-699.
- 691 36. von Hundelshausen P, Weber C. Platelets as immune cells: bridging inflammation and
692 cardiovascular disease. *Circ Res* 2007;**100**:27-40.
- 693 37. Herrler T, Wang H, Tischer A, Schupp N, Lehner S, Meyer A, Wallmichrath J, Habicht A,
694 Mfarrej B, Anders HJ, Bartenstein P, Jauch KW, Hacker M, Guba M. Decompression of
695 inflammatory edema along with endothelial cell therapy expedites regeneration after
696 renal ischemia-reperfusion injury. *Cell Transplant* 2013;**22**:2091-2103.
- 697 38. Gogiraju R, Bochenek ML, Schafer K. Angiogenic Endothelial Cell Signaling in Cardiac
698 Hypertrophy and Heart Failure. *Front Cardiovasc Med* 2019;**6**:20.
- 699 39. Nigam A, Kopecky SL. Therapeutic Potential of Monoclonal Antibodies in Myocardial
700 Reperfusion Injury. *American Journal of Cardiovascular Drugs* 2002;**2**:367-376.
- 701 40. Yellon DM, Hausenloy DJ. Myocardial Reperfusion Injury. *New England Journal of*
702 *Medicine* 2007;**357**:1121-1135.
- 703 41. Davidson SM, Ferdinandy P, Andreadou I, Bøtker HE, Heusch G, Ibáñez B, Ovize M,
704 Schulz R, Yellon DM, Hausenloy DJ, Garcia-Dorado D. Multitarget Strategies to Reduce
705 Myocardial Ischemia/Reperfusion Injury. *Journal of the American College of Cardiology*
706 2019;**73**:89-99.
- 707 42. Weyrich AS, Ma XY, Lefer DJ, Albertine KH, Lefer AM. In vivo neutralization of P-selectin
708 protects feline heart and endothelium in myocardial ischemia and reperfusion injury. *J*
709 *Clin Invest* 1993;**91**:2620-2629.
- 710 43. Schmitt C, Abt M, Ciorciaro C, Kling D, Jamois C, Schick E, Solier C, Benghozi R,
711 Gaudreault J. First-in-Man Study With Inclacumab, a Human Monoclonal Antibody
712 Against P-selectin. *Journal of cardiovascular pharmacology* 2015;**65**:611-619.
- 713 44. Fukushima S. A Novel Strategy for Myocardial Protection by Combined Antibody
714 Therapy Inhibiting Both P-Selectin and Intercellular Adhesion Molecule-1 Via Retrograde
715 Intracoronary Route. *Circulation* 2006;**114**:I-251-I-256.
- 716 45. Tardif JC, Tanguay JF, Wright SR, Duchatelle V, Petroni T, Gregoire JC, Ibrahim R,
717 Heinonen TM, Robb S, Bertrand OF, Cournoyer D, Johnson D, Mann J, Guertin MC,
718 L'Allier PL. Effects of the P-selectin antagonist inclacumab on myocardial damage after
719 percutaneous coronary intervention for non-ST-segment elevation myocardial
720 infarction: results of the SELECT-ACS trial. *J Am Coll Cardiol* 2013;**61**:2048-2055.
- 721 46. Niwa R, Satoh M. The Current Status and Prospects of Antibody Engineering for
722 Therapeutic Use: Focus on Glycoengineering Technology. *Journal of Pharmaceutical*
723 *Sciences* 2015;**104**:930-941.
- 724 47. Chames P, Van Regenmortel M, Weiss E, Baty D. Therapeutic antibodies: successes,
725 limitations and hopes for the future. *Br J Pharmacol* 2009;**157**:220-233.
- 726 48. Riley TR, Riley TT. Profile of crizanlizumab and its potential in the prevention of pain
727 crises in sickle cell disease: evidence to date. *J Blood Med* 2019;**10**:307-311.

728 49. Telen MJ, Wun T, McCavit TL, De Castro LM, Krishnamurti L, Lanzkron S, Hsu LL, Smith
729 WR, Rhee S, Magnani JL, Thackray H. Randomized phase 2 study of GMI-1070 in SCD:
730 reduction in time to resolution of vaso-occlusive events and decreased opioid use. *Blood*
731 2015;**125**:2656-2664.
732

733

FIGURES

734
735
736
737
738
739
740
741
742
743
744
745

746
747
748
749
750
751
752

753
754
755
756
757
758
759
760
761
762

763
764
765
766
767
768
769
770

771
772
773
774
775

Figure 1. One-bead-one-peptide library synthesis. **A)** A combinatorial peptide library was designed using the split synthesis method of Lam et al. biased toward a known E-selectin binding sequence. (1) Resin was split in half; (2) half was coupled to the first amino acid of the selectin binding sequence and the other half divided evenly into 30 tubes, each containing a different amino acid. (3) After coupling was complete, resin was combined and deprotected. (4) The cycle was repeated for each amino acid in the selectin-binding sequence to create a library with 31^7 unique peptide sequences. **B)** In each step, resin is divided in two and coupled to a different amino acid, b_x or a_x . The cycle is repeated three times to create a library with 2^3 unique sequences. **C)** An example of the screening result is shown. Resin with peptide that bound E-selectin can be seen in brown (red arrows). This figure was created with BioRender.

Figure 2. Improved binding to immobilized selectin surfaces with DS-IkL. P- and E-selectin coated surfaces were treated with CF594-DS-IkL (30 μ M, red) or CF594-DS (30 μ M, black). CF594-DS-IkL binding increased with increasing concentration, as assessed by mean fluorescence intensity (MFI) normalized to vehicle (HBSS). Data are represented as means \pm SEM of 3 biological replicates. * $p < 0.05$, ** $p < 0.01$, *** $p < 0.001$ by two-way ANOVA with post-hoc Tukey test.

Figure 3. Treatment with DS-IkL reduced neutrophil binding and platelet activation. Platelet activation on stimulated HCMECs as assessed by **A)** NAP-2 and **B)** PF-4 was reduced after treatment with DS-IkL (30 μ M) and/or IkL peptide (450 μ M), but not DS (30 μ M). $n=3$ biological replicates. **C)** E-selectin coated microspheres were treated with HBSS, DS-IkL, IkL peptide, or DS prior to incubation with isolated human neutrophils (PMN). Data represent PMN binding to microspheres as assessed by flow cytometry. $n=3-6$ biological replicates. **D)** DS-IkL reduced PMN binding to stimulated HCMECs toward the level of unstimulated controls ($p=0.09$). $n=3-4$ biological replicates. All data are represented as means \pm SEM. * $p < 0.05$, ** $p < 0.01$, *** $p < 0.001$ by one-way ANOVA with post-hoc Tukey test.

Figure 4. DS-IkL targeted to the heart after I/R. Animals were injected with either CF594 dissolved in saline or CF594-DS-IkL after surgery and 24 hours later. **A)** Representative images taken 1 hour after each injection, and every 12 hours after reperfusion until the 36-hour time point. **B)** Data summary of CF594 (black bars) and CF594-DS-IkL (red bars) targeting to heart at 1, 12, 24, and 36 hours after surgery. Black arrows depict injections. Data are represented as means \pm SEM of $n=6$ mice per group. * $p < 0.05$, ** $p < 0.01$; *** $p < 0.001$ by two-way ANOVA with post-hoc Tukey test.

Figure 5. Mice treated with DS-IkL exhibited reduced infarct size and improved cardiac function after I/R. **A)** After 24 hours of reperfusion, we assessed size of myocardial infarction using TTC staining. Representative sections are shown. **B)** Quantification revealed an increase in infarct size with saline treated mice. **C)** Cardiac injury was also assessed using cardiac troponin I.

776

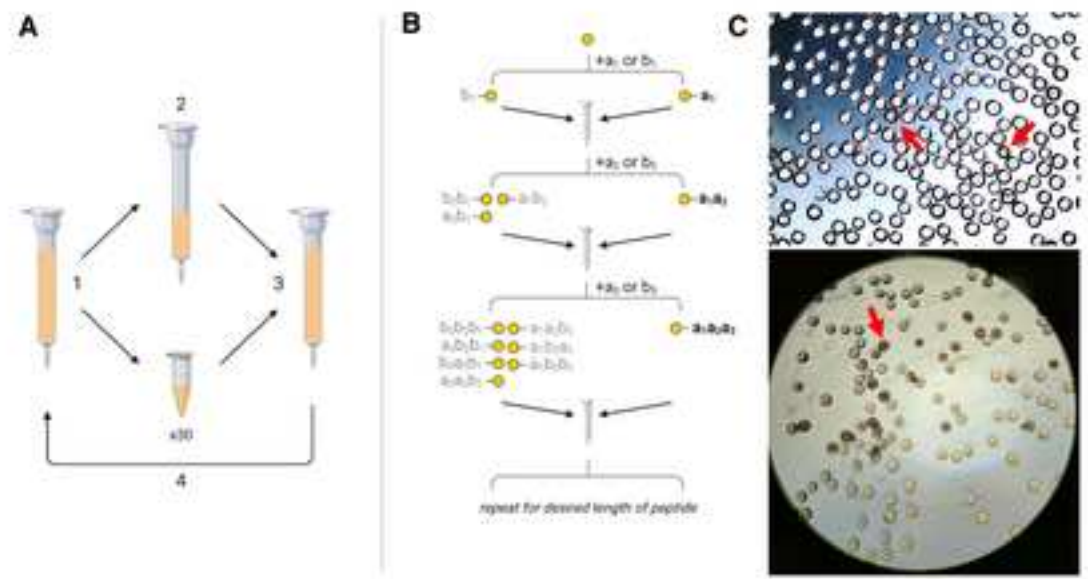
777 After 2 weeks of reperfusion, mice were subjected to conscious echocardiography to examine the
778 cardiac structure and function. **D)** Representative M-mode images at the parasternal short-axis for
779 all four groups are depicted. **E)** Heart rate was not significantly different in these conscious mice.
780 **F)** I/R induced an increase in left ventricular (LV) mass, and **G)** reduced fractional shortening and
781 **H)** global radial strain. **I)** Summary data of region-specific radial strain and **J)** circumferential
782 strain are displayed. **K)** Diastolic function was assessed by the blood flow velocity through the
783 mitral valve, as shown in representative images in all four groups. **L)** The E/A ratio was
784 significantly decreased in both groups but was more obvious in the saline I/R group. **M)** Although
785 the isovolumetric relaxation time (IVRT) was not significantly different in all four groups, **N)** there
786 was a difference in the mitral valve (MV) deceleration time in the saline I/R group vs the saline
787 sham group. In each graph, data are represented as means \pm SEM of n=5-7 mice per group. *
788 $p < 0.05$, ** $p < 0.01$ by one-way ANOVA with post-hoc Tukey test.

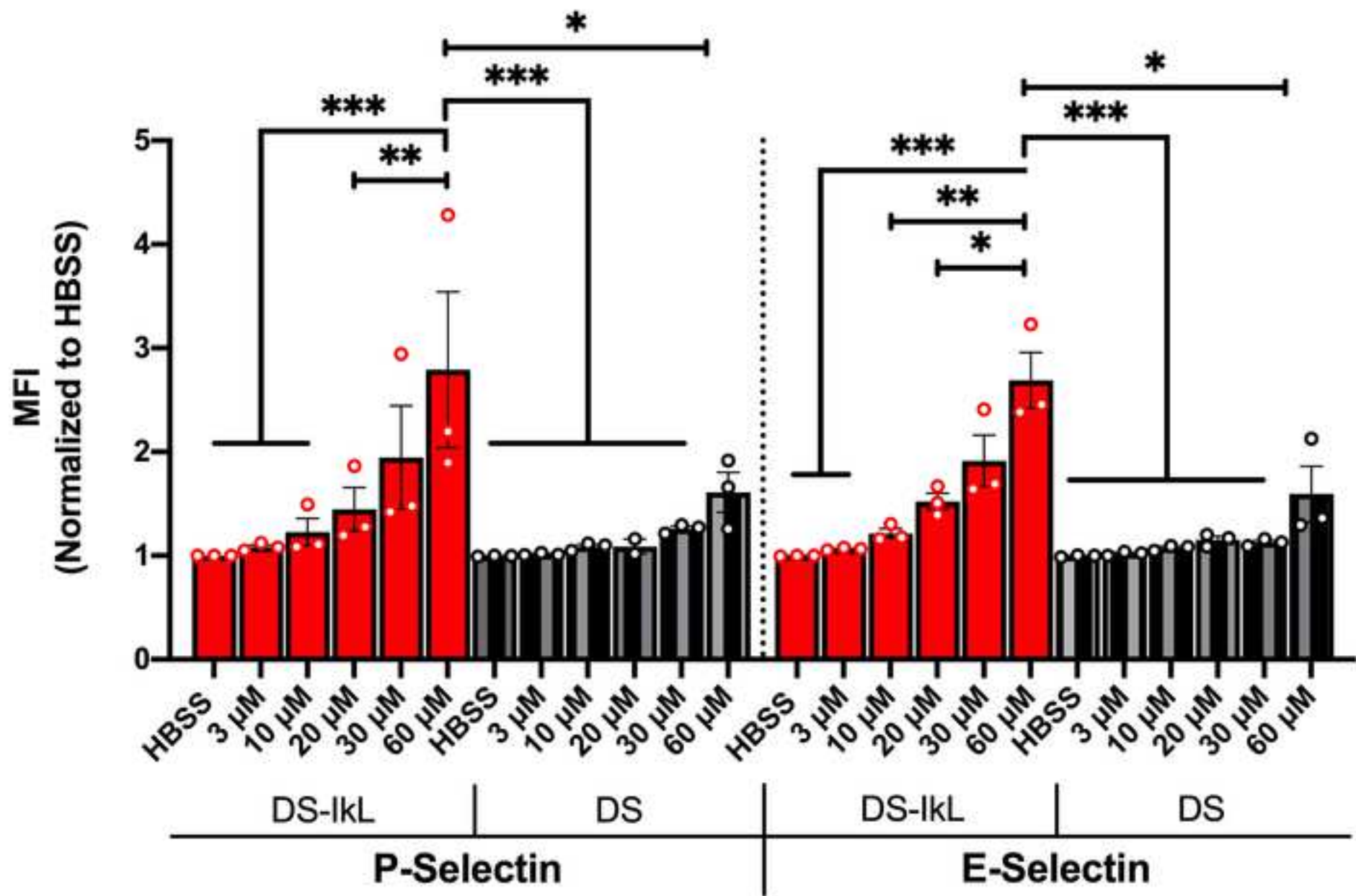
789

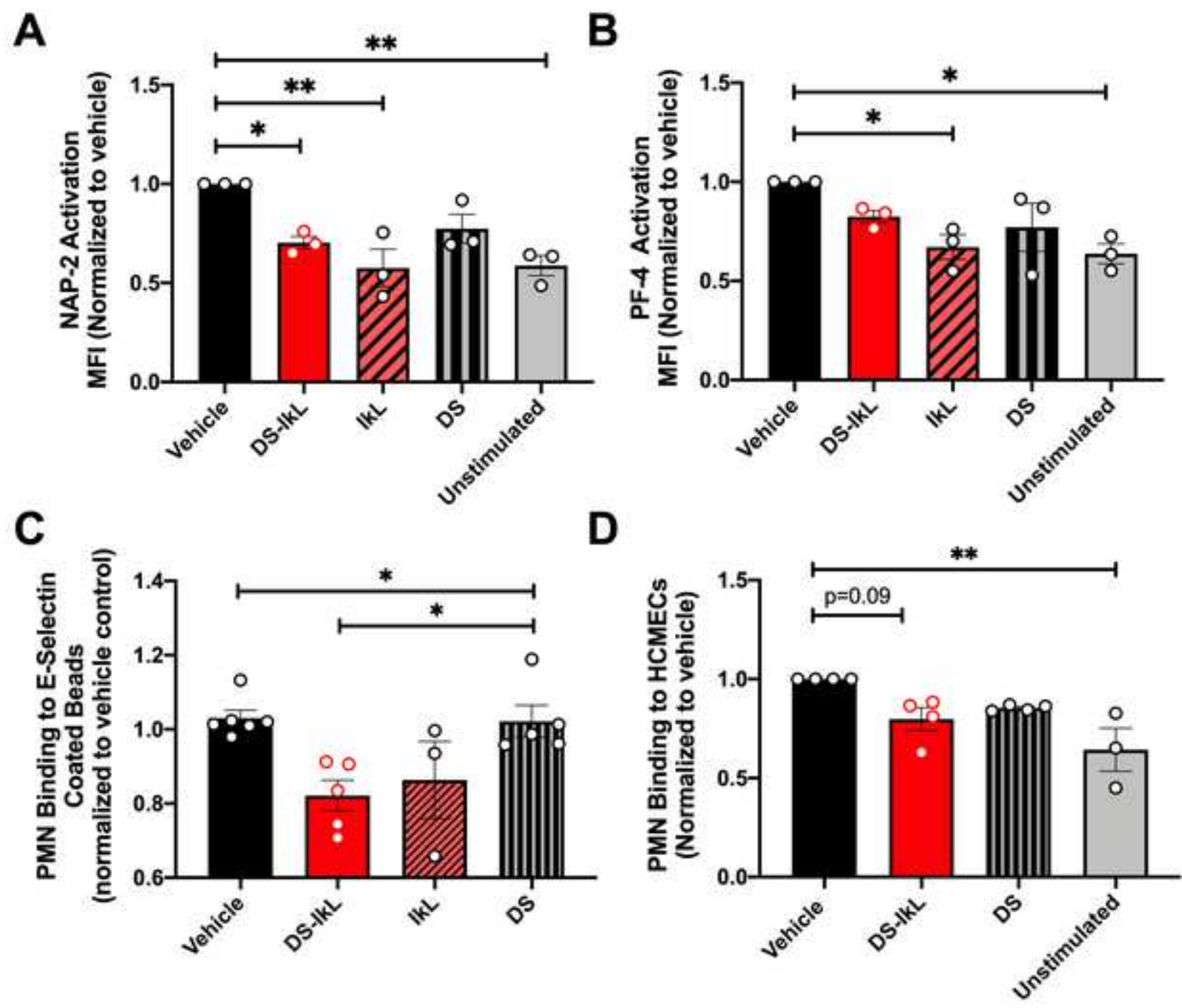
790 **Figure 6. DS-IkL limited fibrosis after I/R.** **A)** Representative images of whole hearts (top),
791 Masson's Trichrome (middle), and Picrosirius Red (bottom) stained sections. Collagen deposition
792 by Masson's Trichrome (**B and C**) and Picrosirius Red (**D and E**) was significantly reduced in
793 DS-IkL treated mice after I/R. Data are represented as means \pm SEM of n=5-7 mice per group;
794 datapoints display 2-4 sections analysed per mouse. * $p < 0.05$, ** $p < 0.01$, *** $p < 0.001$ by one-
795 way ANOVA with post-hoc Tukey test.

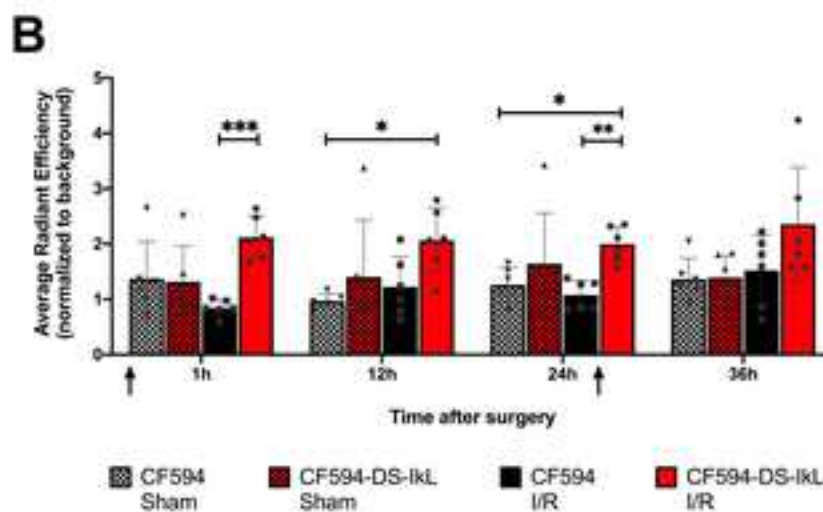
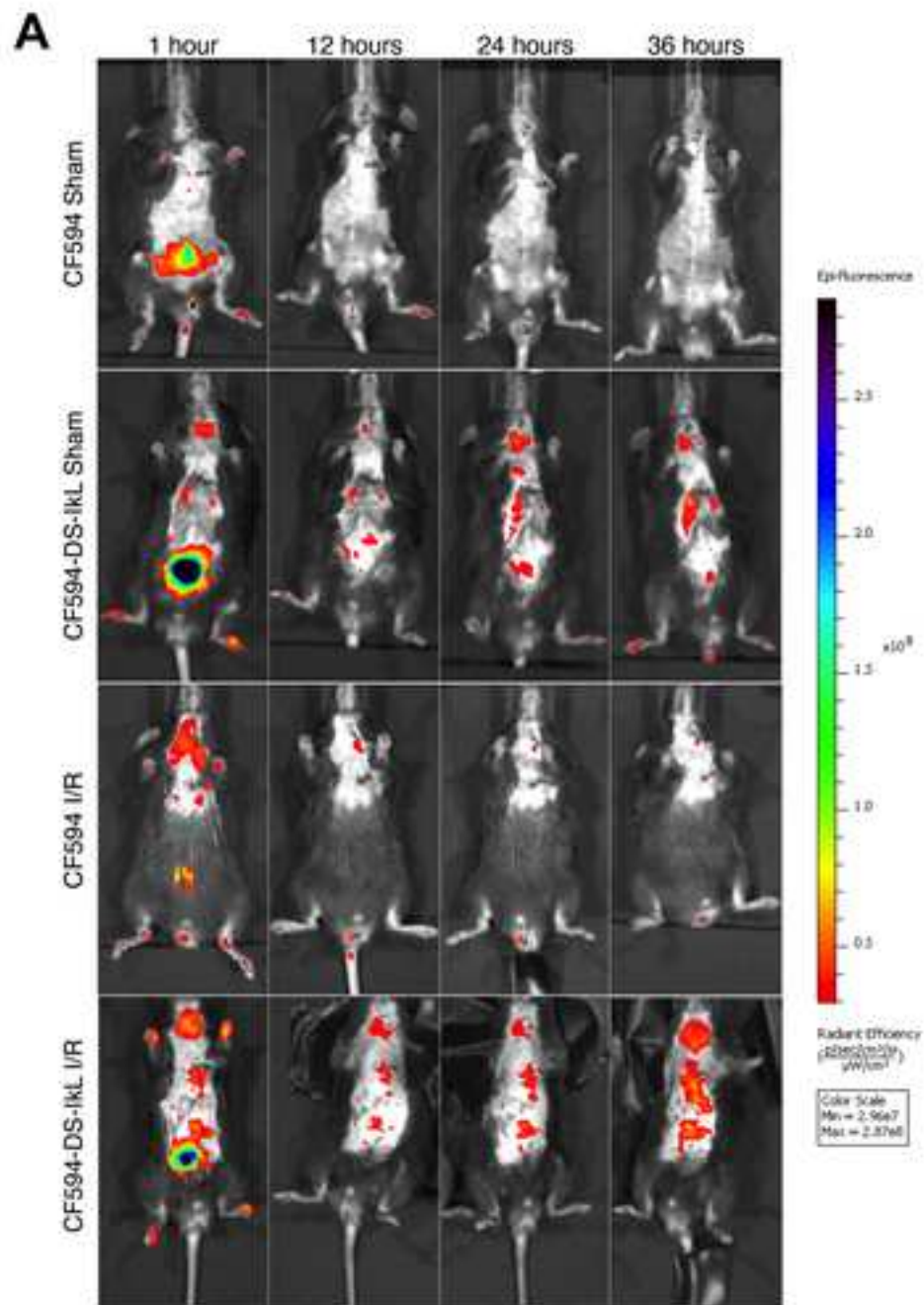
796

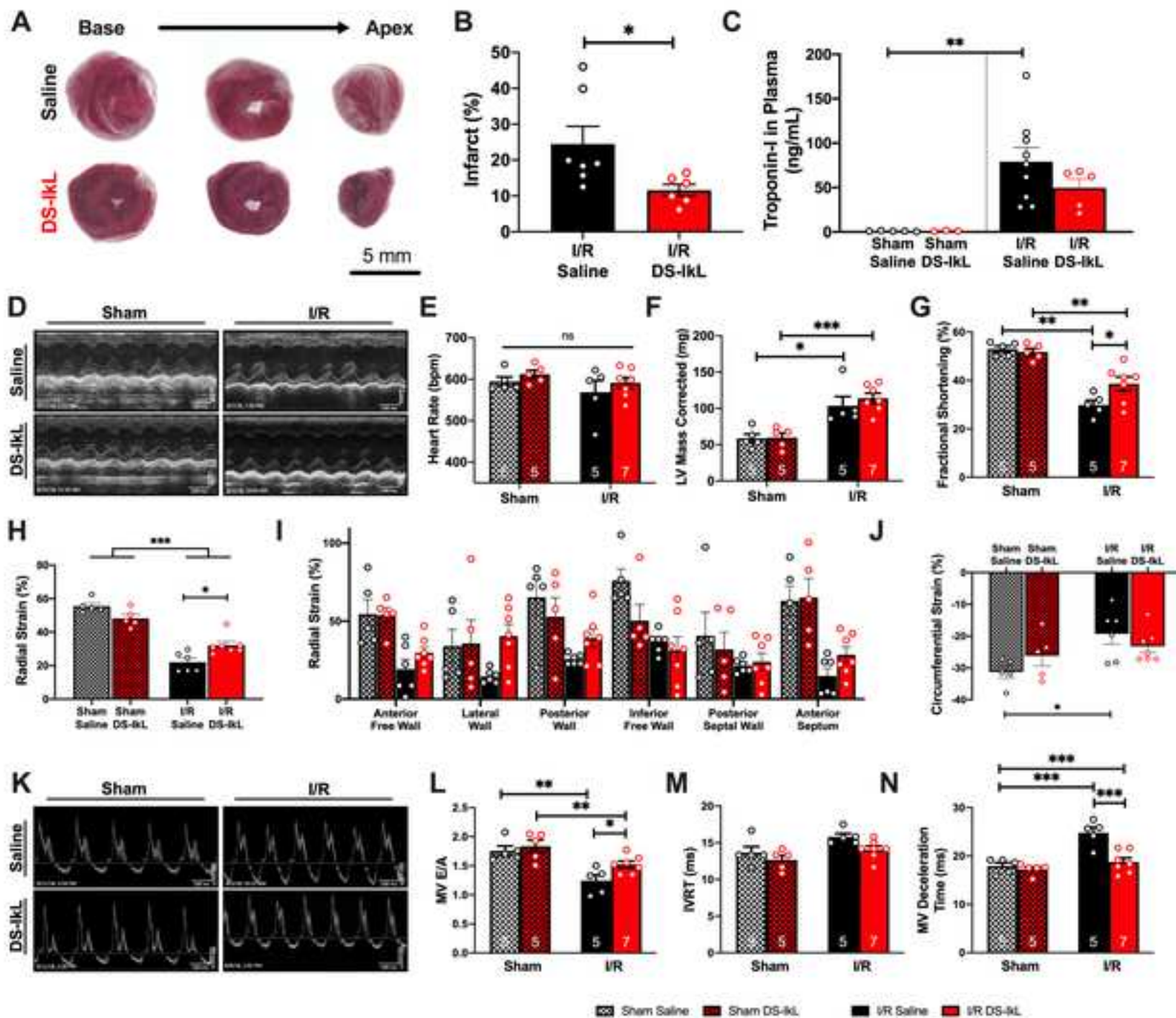
797 **Figure 7. DS-IkL prevented neutrophil and macrophage aggregation, fibroblast**
798 **proliferation, and endothelial cell proliferation after I/R.** We investigated the short- and long-
799 term effects of DS-IkL on the immune response. **A)** Flow cytometric analysis of isolated cardiac
800 cells. Nucleated cells were selected from debris based on the incorporation of 7-ADD and the
801 separation of the myocytes from the non-myocyte cells (NMC) using a cardiac myosin heavy chain
802 (MF20)-specific antibody. Neutrophils and monocytes were separated based on the presence of
803 CD11b/Lys6-C/G from all four groups as depicted. Neutrophils were further distinguished by
804 gating on the SSC-high and FSC-low cells from CD11b⁺/Ly6C/G⁺ population. **B)** Summary data
805 shows that there was a significant reduction in neutrophils in the DS-IkL I/R group, compared to
806 the saline I/R group. 3 technical replicates per mouse are shown. **C)** Flow cytometric analysis of
807 CD31⁺/Thy1.2⁻ endothelial cells in all four groups. **D)** Summary data showing a significant
808 increase in endothelial cells in saline I/R group relative to saline sham. DS-IkL prevented the
809 increase. Data show 2 technical replicates per mouse. **E)** Assessment of proliferation using the
810 Ki67 proliferative marker showed a similar trend. Data represent averages of 2 technical replicates
811 per mouse. **F)** Fibroblasts (Thy1.2⁺/CD11b⁻/Ly6C/G⁻) were detected using flow cytometric
812 analysis. **G)** Summary data of Thy1.2 positive cells (2 technical replicates per mouse) and **H)**
813 proliferative Thy1.2 positive cells using Ki67 (averages of 2 technical replicates per mouse) are
814 shown. X and Y axes represent arbitrary units. **I)** We examined the accumulation of neutrophils
815 (Ly6G) and macrophages (F4/80) after 2 weeks of I/R using IHC. Representative images are
816 shown for all four groups. DS-IkL prevented accumulation of both **J)** macrophages and **K)**
817 neutrophils. n=3-5 mice per group for flow cytometric analysis. n=3 mice per group, 2-3 sections
818 per mouse for IHC. Data are represented as means \pm SEM. * $p < 0.05$, ** $p < 0.01$, *** $p < 0.001$ by
819 one-way ANOVA with post-hoc Tukey test.

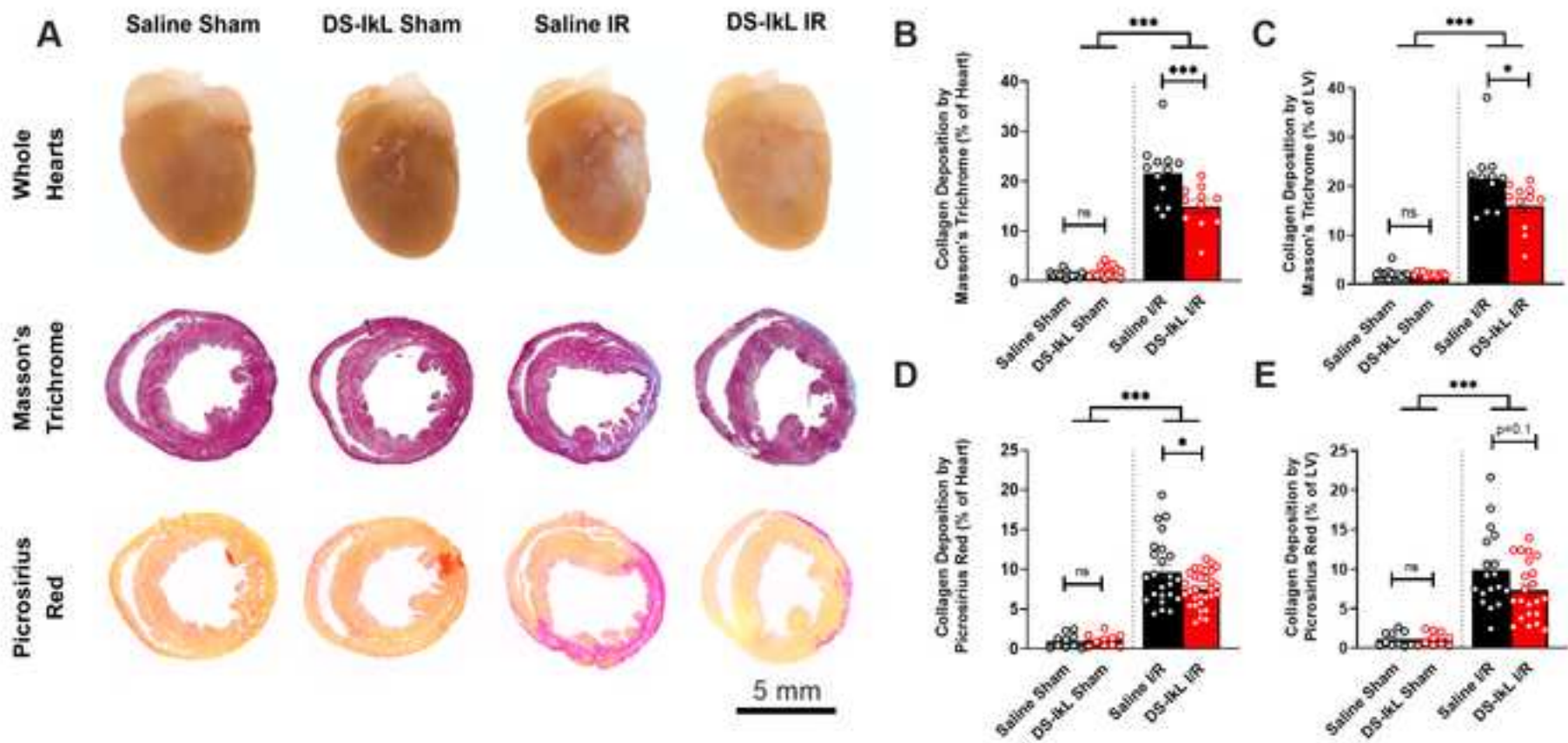


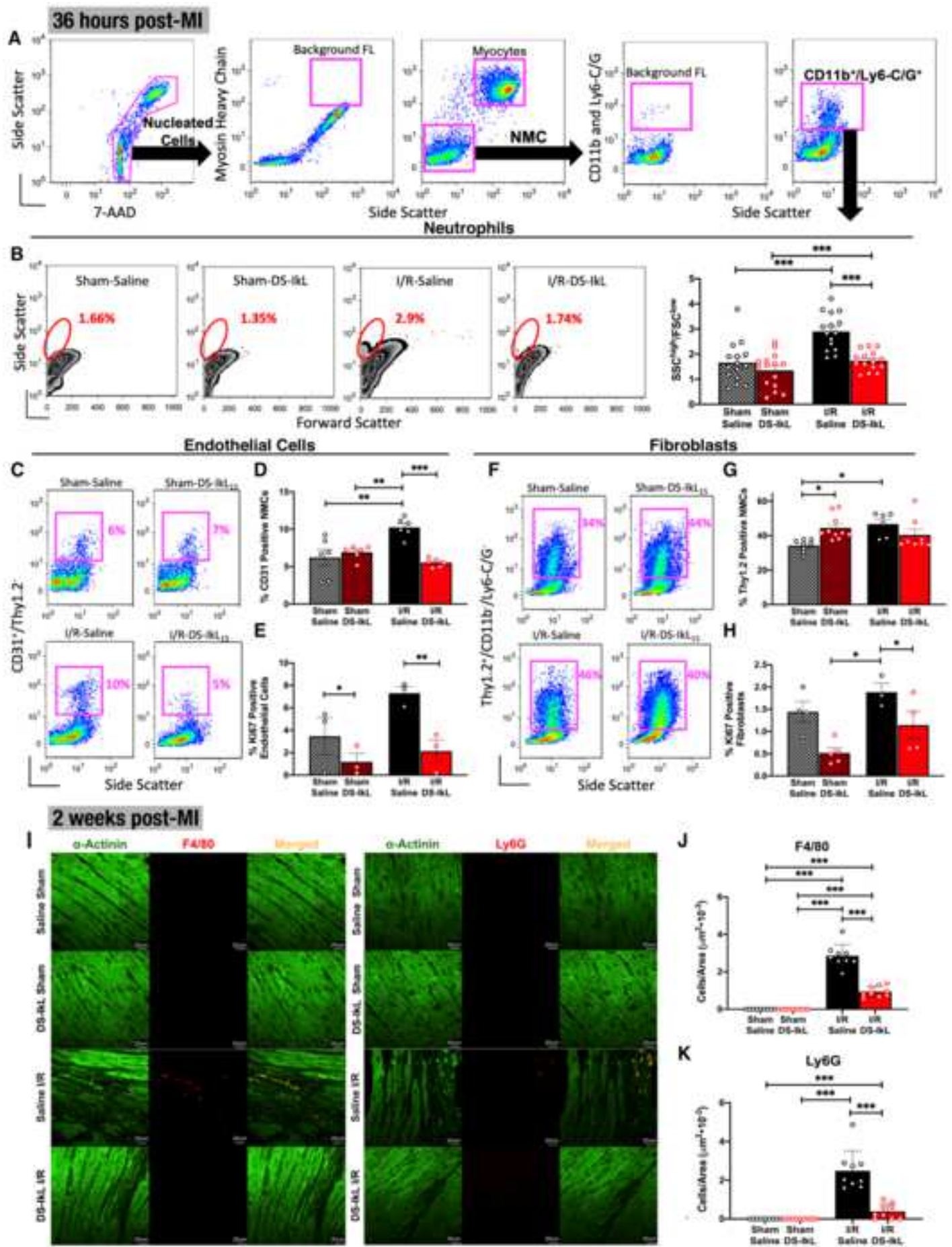


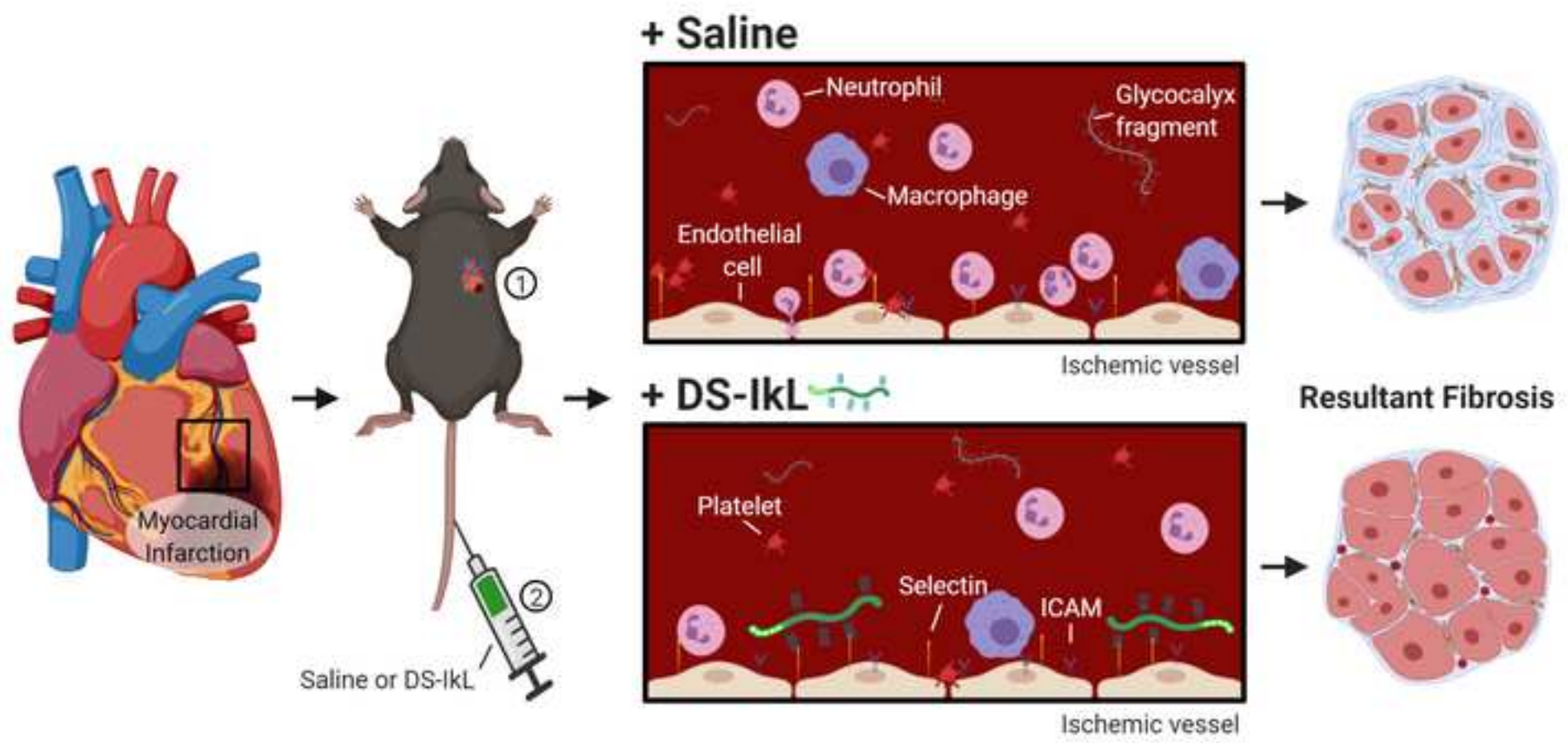












Selectin-Targeting Glycosaminoglycan-Peptide Conjugate Limits Neutrophil Mediated Cardiac Reperfusion Injury

Tima Dehghani^{1*}, Phung N. Thai^{2*}, Harkanwalpreet Sodhi¹, Lu Ren², Padmini Sirish², Carol E. Nader², Valeriy Timofeyev², James L. Overton², Xiaocen Li³, Kit S. Lam³, Nipavan Chiamvimonvat^{2,4,5}, Alyssa Panitch¹

¹Department of Biomedical Engineering, University of California, Davis

²Department of Internal Medicine, Division of Cardiovascular Medicine, University of California, Davis

³Department of Biochemistry and Molecular Medicine, University of California, Davis

⁴Department of Veterans Affairs, Northern California Health Care System, Mather, CA

⁵Department of Pharmacology, University of California, Davis

*Authors contributed equally to this project

Short Title: Glycocalyx mimic limits cardiac reperfusion injury

Supplementary Materials

Methods

Peptide Library

1 g of resin was swollen in dimethylformamide (DMF) overnight and divided in half. Half of the resin was coupled to the first amino acid in the known sequence; the other half was split equally into 30 polypropylene columns, each containing a different amino acid (10 equivalents in DMF). Ten equivalents of N-N'-diisopropylcarbodiimide (DIC) and hydroxybenzotriazole (HOBt) were added. Complete coupling was confirmed by a colorless Kaiser test. The resin was then combined into a single column and deprotected with 20-25% piperidine. The process was repeated for the next amino acid in the known sequence.

Library Screening for E-Selectin Binding Peptide

Peptide-conjugated Tentagel S resin was immobilized with 90% DMF to form a confluent monolayer on a 12-well polystyrene plate. Resin was blocked with 5% bovine serum albumin (BSA) in phosphate buffered saline (PBS) then pre-screened for binding to the HRP-anti-His secondary antibody (1:400 in PBS, 1 hour at room temperature with rocking). Resin which stained positive was removed prior to screening. Resin was then blocked with a human FC fragment (1mg/ml in 1% BSA) for 1 hour at room temperature with rocking. FC-chimera human recombinant E-selectin with a 6-histidine tag (R&D Systems) was added to each well and incubated overnight at 4°C with rocking, washed 3x with PBS, then treated with HRP-anti-His for 1 hour at room temperature. Resin was washed and visualized using a 3,3' diaminobenzidine (DAB) solution. Resin which stained positive for E-selectin binding was removed and sequenced. This procedure was repeated until 30 unique sequences were identified. Sequences were compared

for homology and multiple selected for further analysis. Sequences were remade on Tentagel S resin and binding to E-selectin compared.

DS-IkL inhibiting selectin and ICAM binding to neutrophils

Isolated neutrophils were resuspended in HBSS^{+/+} with 0.4% HSA and added at 165k cells per tube. DS-IkL was dissolved in HBSS^{+/+} at 120 uM, sterile filtered through a 0.2 um filter, and serially diluted to 60 uM, 30 uM, and 10 uM. Fifty microlitres of DS-IkL was added to a 1.5 mL Eppendorf tube containing 40 uL of the neutrophil suspension, followed by 10 uL of 100 ug/mL recombinant human ICAM, P-selectin, or E-selectin. This yielded final DS-IkL concentrations of 60 uM, 30 uM, 15 uM, and 5 uM and 10 ug/mL selectin. For stimulated groups, TNF- α was added to samples at a final concentration of 5 ng/mL. Tubes were gently mixed then incubated on ice with rotation (120 RPM). After 30 minutes samples were washed twice with HBSS^{+/+} then blocked with 5% BSA in HBSS^{+/+} + 5mM HEPES for 60 minutes. Samples were stained with PE anti-human CD62E, PE anti-human CD62P, or PE anti-human CD54 antibodies (BioLegend, San Diego, CA) for 30 minutes (4 uL antibody per 100 uL solution), washed twice, then immediately ran on an Attune NxT Flow Cytometer. Data was analysed in FlowJo by plotting SSC-A versus FSC-A and selecting the granulocyte population, excluding doublets by plotting FSC-A versus FSC-H, then gating for PE+ populations compared to unstained controls.

Troponin I Measurements

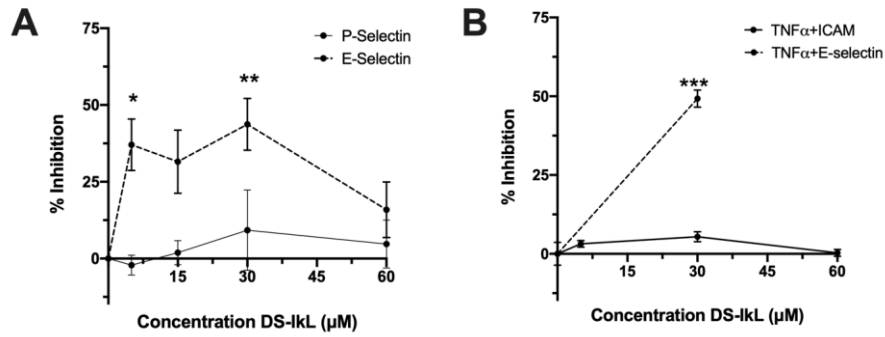
Mice were injected with heparin before they were sacrificed. After removal of hearts, blood was collected into EDTA-coated blood tubes and spun down at 2000xg for 30 mins. Separated plasma was transferred into a new tube and flash frozen. Troponin I (CNTI) was measured using a commercial kit (Life Diagnostics). Plasma was thawed then centrifuged at 2000xg for 20 minutes

at 7°C. Supernatant was diluted 1:4 in plasma diluent, then further diluted in standard diluent as needed (final dilution 1:8 or 1:12). Standards were prepared by serially diluting a CNTI stock solution to 10, 5, 2.5, 1.25, 0.625, 0.313, and 0.156 ng/mL. HRP conjugate (100 µL) was added to anti-CTNI coated wells followed by 100 µL of standards or diluted plasma, each ran in duplicate. Wells were incubated on an orbital micro-plate shaker at 150 rpm and room temperature for one hour. Wells were emptied and washed 6x with 1x wash solution. TMB chromogen (100 µL) was added and incubated for 15 minutes at 150 rpm and room temperature. Stop solution (100 µL) was added to each well and absorbance measured immediately at 450 nm. Sample concentrations were extrapolated from a standard curve generated in GraphPad Prism (San Diego, CA) using 4-parameter logistic regression. Sample concentrations were multiplied by their respective dilution factors to obtain final concentration values.

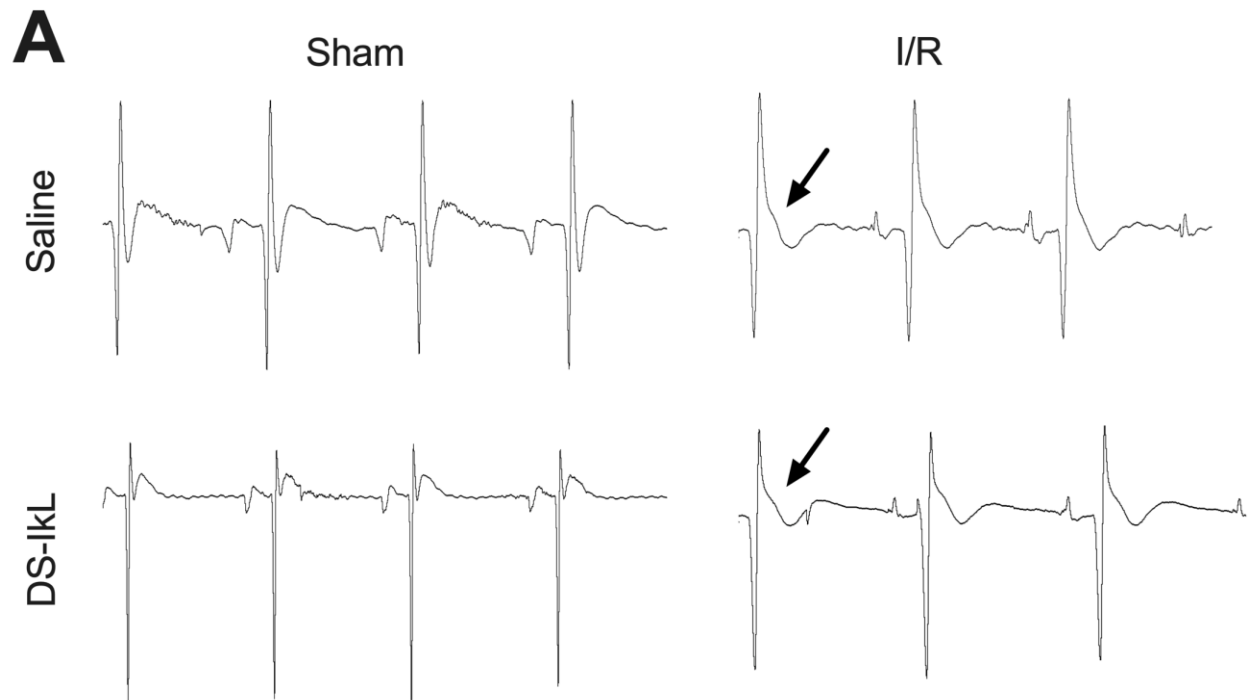
Cell Isolation

Mice were injected with 0.1 ml heparin (1000 units/ml) 10 mins prior to heart extraction. Mice were anesthetized with ketamine/xylazine (80 mg/kg / 5 mg/kg). Hearts were removed and placed in Tyrode's solution containing in mM: 140 NaCl, 5.4 KCl, 1.2 MgCl₂, 5 N-2-hydroxyethylpiperazine-N'-2-ethanesulphonic acid (HEPES), and 5 glucose at a pH 7.4. The aorta was cannulated, mounted on a Langendorff setup, and retrogradely perfused with Tyrode's solution containing O₂ at 37°C for 3 mins at a flow rate of approximately 3 ml/min. The perfusion pressure was monitored, and the flow rate was adjusted to maintain perfusion pressure at ~80 mmHg. The solution was then switched to Tyrode's solution containing collagenase type 2 (1 mg/ml, 330 units/mg, Worthington Biochemical Corporation). After about 12 mins of enzyme perfusion, hearts were removed from the perfusion apparatus and gently separated in high K⁺

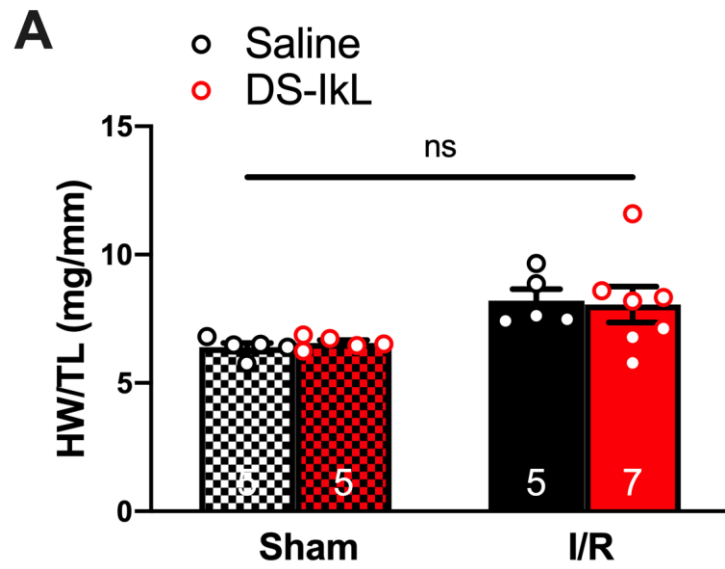
solution containing in mM: 120 potassium glutamate, 20 KCl, 1 MgCl₂, 0.3 EGTA, 10 glucose, and 10 HEPES, pH 7.4 with KOH. All chemicals were acquired from Sigma Chemicals (St. Louis, MO) unless stated otherwise.



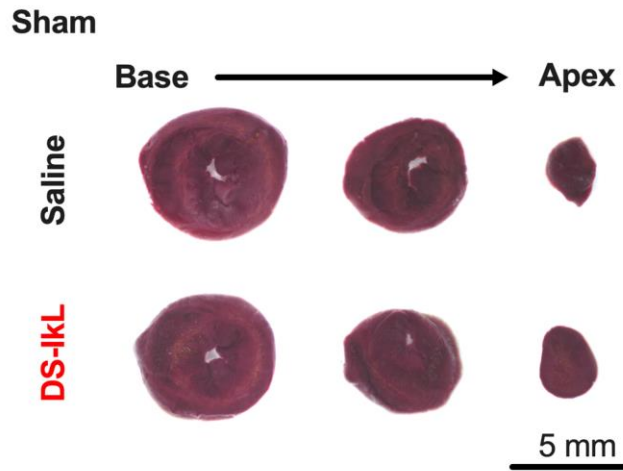
Supplementary Figure 1. A) Neutrophils bound less E-selectin, but not P-selectin, in the presence of 5, 15, and 30 uM DS-IkL. **B)** Under stimulatory conditions (5ng/mL TNF- α), 30 uM of DS-IkL had no effect on neutrophil binding to ICAM. Data are represented as means \pm SEM of 3 biological replicates. * $p < 0.05$, ** $p < 0.01$, *** $p < 0.001$ by one-way ANOVA with post-hoc Tukey test.



Supplementary Figure 2. A) Representative ECG recordings during surgical procedure. For I/R mice, confirmation of LAD ligation was done visually (blanching of the heart) and also by the presence of ST-elevation.



Supplementary Figure 3. A) Heart weight normalized to tibial length of all four groups. n=5-7 mice per group.



Supplementary Figure 4. Representative heart sections from sham-operated mice after TTC staining. Sections were taken from base to apex. n=5 mice per group.

Supplementary Table 1. Echocardiography Table

	Saline Sham (n=5)	DS-IkL Sham (n=5)	Saline I/R (n=6)	DS-IkL I/R (n=7)	p-value: Saline I/R vs DS-IkL I/R
Heart Rate (bpm)	580±3	612±10	569±28	591±13	NS
LV Mass Corr (mg)	58.6±6.0	59.8±6.4	103.6±12.6	113.9±7.1	NS
LVAW;d (mm)	0.77±0.02	0.78±0.07	0.90±0.06	0.86±0.02	NS
LVAW;s (mm)	1.43±0.05	1.44±0.09	1.39±0.10	1.54±0.04	NS
LVID;d (mm)	3.12±0.07	3.17±0.13	3.91±0.28	3.85±0.20	NS
LVID;s (mm)	1.41±0.05	1.53±0.09	2.76±0.24	2.41±0.25	NS
LVPW;d (mm)	0.76±0.04	0.78±0.05	0.85±0.06	0.87±0.04	NS
LVPW;s (mm)	1.38±0.08	1.45±0.11	1.21±0.11	1.48±0.09	NS
CO (ml/min)	20.1±1.1	20.1±2.3	22.1±4.4	25.4±1.8	NS
Ejection Fraction (%)	86.5±1.1	83.5±1.4	57.4±3.1	68.2±4.4	<0.05
Fractional Shortening (%)	54.8±1.3	51.8±1.4	29.8±2.0	38.1±3.2	<0.05
LV Vol;d (µl)	38.7±1.9	40.5±4.3	68.6±12.7	65.5±8.5	NS
LV Vol;s (µl)	5.8±0.4	6.5±0.9	29.9±6.6	22.8±6.4	NS
Stroke Volume (µl)	34.3±1.8	32.7±3.4	38.4±6.7	42.9±2.9	NS
Radial Strain (%)	55.5±1.83	48.25±2.4	22.0±2.4	32.19±2.2	<0.05
Circumferential Strain (%)	-31.3±1.9	-26.2±3.2	-19.3±3.2	-23.2±2.0	NS
IVRT	13.67±0.8	12.7±0.6	15.8±0.5	14.1±0.5	NS
MV E/A	1.77±0.08	1.84±0.1	1.24±0.1	1.52±0.06	<0.05
MV Deceleration Time (s)	17.89±0.7	17.2±1.2	24.8±1.6	18.7±0.9	<0.001

Supplementary Table 2: Commercial Reagent List

<u>Reagent/Antibody</u>	<u>Vendor</u>	<u>Location</u>	<u>Catalog Number</u>
PE anti-human CD62E antibody, clone HCD62E	BioLegend	San Diego, CA, USA	322606
PE anti-human CD62P antibody, clone AK4	BioLegend	San Diego, CA, USA	304906
Dermatan Sulfate	Celsus Labs	Cincinnati, OH, USA	
Recombinant human E-selectin-FC chimera protein	R&D Systems	Minneapolis, MN, USA	724-ES-100
Recombinant human P-selectin-FC chimera protein	R&D Systems	Minneapolis, MN, USA	137-PS-050
EasySep™ Direct Human Neutrophil Isolation Kit	StemCell Technologies	Cambridge, MA, USA	19666
PE anti-human CD54 antibody, clone HA58	BioLegend	San Diego, CA, USA	353106
Human Cardiac Microvascular Endothelial Cells	PromoCell	Heidelberg Germany	C-12285
Endothelial growth medium MV	PromoCell	Heidelberg Germany	C-22120
Calcein-AM	BioLegend	San Diego, CA, USA	425201
Human Serum Albumin Solution – 25%	Gemini Bio		800-120
AF488 anti-human CD11a/CD18, clone m24	BioLegend	San Diego, CA, USA	363404
PE anti-human CD15, clone HI98	BioLegend	San Diego, CA, USA	301906
CF594 Dye Hydrazide	Biotium	Fremont, CA, USA	92158
Prostaglandin E1	Enzo Life Sciences	Farmingdale, NY, USA	BML-PG006-0010
Solid state peptide synthesis products	CEM and AAPPTec		Various
4-(4,6-Dimethoxy-1,3,5-triazin-2-yl)-4-methylmorpholinium chloride	Sigma-Aldrich	St. Louis, MO, USA	74104-1G-F
Human CXCL7/NAP-2 Antibody	R&D Systems	Minneapolis, MN, USA	MAB393
Human CXCL7/NAP-2 Biotinylated Antibody	R&D Systems	Minneapolis, MN, USA	BAF393
Human CXCL4/PF4 Antibody	R&D Systems	Minneapolis, MN, USA	AF795

Human CXCL4/PF4 Biotinylated Antibody	R&D Systems	Minneapolis, MN, USA	BAF795
EDTA Solution	Promega	Madison, WI, USA	V4231
Theophylline	Sigma-Aldrich	St. Louis, MO, USA	T1633-100G
PolyLink Protein Coupling Kit	PolySciences, Inc.	Warrington, PA, USA	24350-1
Fluoresbrite® 641 Carboxylate Microspheres 1.75µm	PolySciences, Inc.	Warrington, PA, USA	17797
Pierce™ Recombinant Protein A/G	ThermoFisher	Waltham, Massachusetts, USA	21186
BS3 (bis(sulfosuccinimidyl)suberate)	ThermoFisher	Waltham, Massachusetts, USA	21580
Thy1.2-PE antibody	e-Bioscience	San Diego, CA, UCSA	12-0902-81
Rat Anti-Mouse CD11b antibody	BD Bioscience	Franklin Lakes, NJ, USA	557397
Rat Anti-Mouse Ly-6C/G antibody	BD Bioscience	Franklin Lakes, NJ, USA	553128
MyHC antibody	Developmental Studies Hybridoma Bank	Iowa City, IA, USA	
Rat Anti-Mouse CD31 antibody	BD Bioscience	Franklin Lakes, NJ, USA	558737
Rat Anti-Mouse Ki-67 antibody	BD Bioscience	Franklin Lakes, NJ, USA	558615
Mouse Cardiac Troponin-I ELISA	Life Technologies	West Chester, PA, USA	CTNI-1 HSP